UCDAVIS

UCDAVIS AGGIES

Monte Carlo Simulations for Ultra Cold Atoms

1. Motivation: Strongly Correlated Phases of Matter
2. The Hubbard Hamiltonian
3. Classical Monte Carlo
4. World Line Quantum Monte Carlo (Bosonic atoms)
5. Determinant Quantum Monte Carlo (Fermionic atoms)
6. Why Ultracold Atoms?
7. Outlook

Main goals:

How QMC works

Overall sense for capabilities and limitations of QMC

Find me at "Wonder Room"

Or contact via email: scalettar@physics.ucdavis.edu.

Acknowledgement: DOE DE-SC0014671

0. Determinant Quantum Monte Carlo Code

If you are interested, send me an email and I will send:

- DQMC code
- Description of how to run and interpret output
- Code for analytic check at $U = 0$ (free fermions)
- Code for analytic check at $t = 0$ (single cite limit)

We can discuss during "Wonder Room" hours.

1. Motivation: Strongly Correlated Phases of Matter

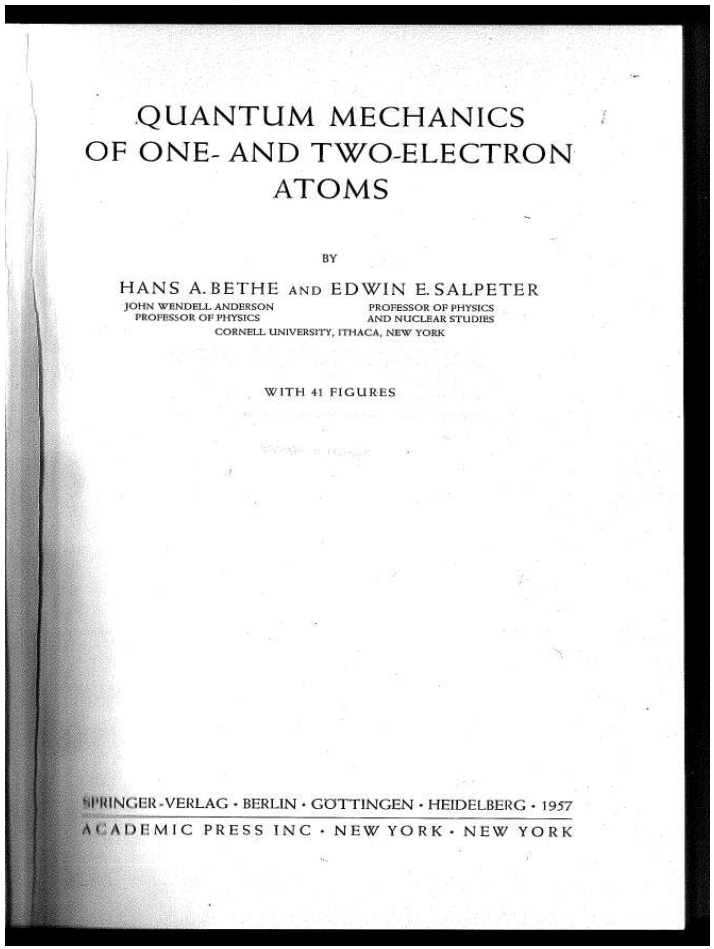

QUANTUM MECHANICS
OF ONE- AND TWO-ELECTRON
ATOMS

BY

HANS A. BETHE AND EDWIN E. SALPETER

JOHN WENDELL ANDERSON PROFESSOR OF PHYSICS
PROFESSOR OF PHYSICS AND NUCLEAR STUDIES
CORNELL UNIVERSITY, ITHACA, NEW YORK

WITH 41 FIGURES

SPRINGER-VERLAG · BERLIN · GÖTTINGEN · HEIDELBERG · 1957
ACADEMIC PRESS INC · NEW YORK · NEW YORK

The aim of this book is two-fold. First, to act as a reference work on calculations pertaining to hydrogen-like and helium-like atoms and their comparison with experiment. However, these calculations involve a vast array of approximate methods, mathematical tricks, and physical pictures $\cdots$.

For atoms and ions with two electrons, such as H^-, He, Li^+, etc., exact analytic solutions are not possible at the present time $\cdots$. (1957, three decades after the invention of quantum mechanics, and still true today!)

What shall we do with solids with 10^{23} electrons?!?!

Origin of Energy Bands in a Solid (noninteracting HM)

Individual atoms: discrete energy levels

Atoms far apart: electrons are localized on single atom

Atoms brought together (solid): degenerate level couple and broaden into a band.

Eigenvectors are delocalized (plane/"Bloch" waves)

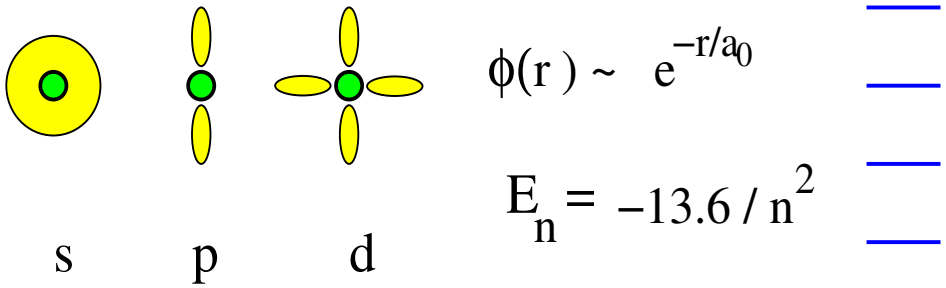

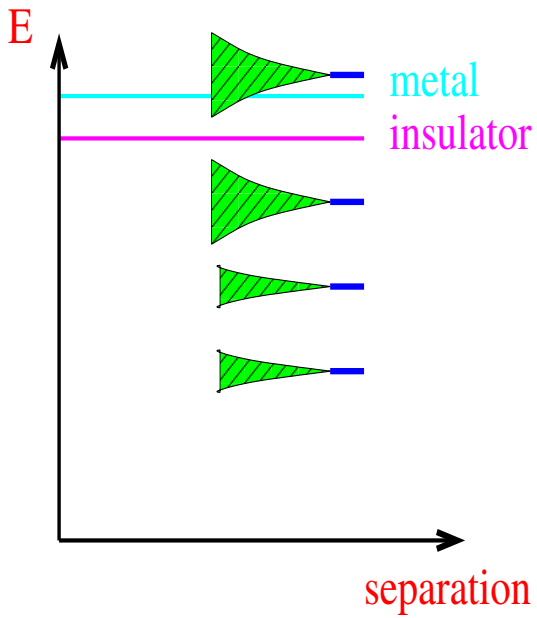

Metals and Band Insulators

Energy band completely filled: Insulator

Finite energy gap to next unoccupied level

Simple counting arguments predict whether many solids are metallic or insulating!!

k eigenstate can be occupied by two electrons (spin $\uparrow, \downarrow$).

Solids with an odd number of electrons per unit cell must be metallic.

Alkalis (Li, Na, K):
one valence e^-
$(2s^1, 3s^1, 4s^1)$ per unit cell:
Good metals.

Diamond, silicon, germanium (C, Si, Ge):
eight valence electrons
$(2s^2 2p^2, 3s^2 3p^2, 4s^2 4p^2)$: per unit cell
Insulators.

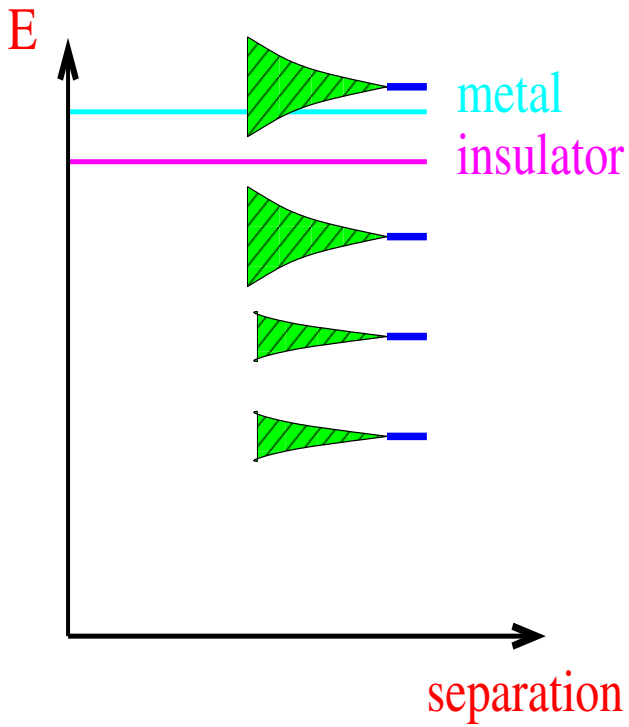

Parent compounds of cuprate superconductors:

- 1 hole/Cu
- Fermi level cuts middle of band.
- Why are they antiferromagnetic insulators?!

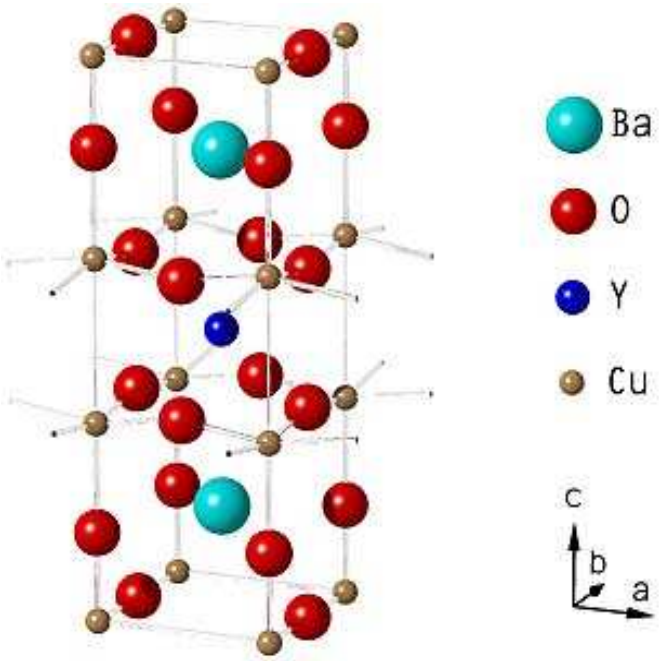

Transition metal monoxides (MnO, FeO, CoO):

(Many oxides in earth's interior.)

MnO: Mn^{2+} d band half-filled (d^5: odd # electrons)

- Why are they antiferromagnetic insulators?!

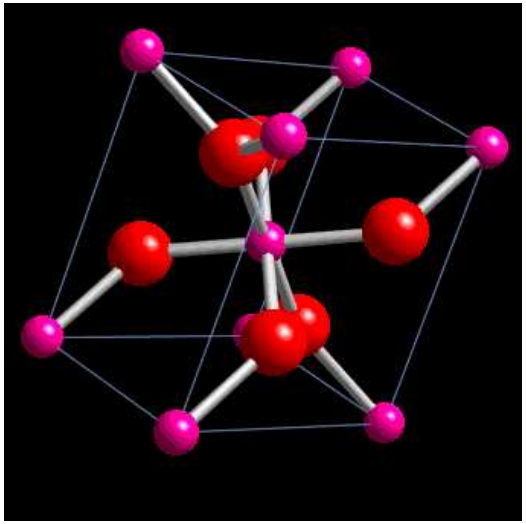

Can however make MnO have the expected metallic behavior...

Diamond Anvil Cell

Apply pressure (and lots of it!) to push atoms closer.

* Direct measurement of resistance
* Probe magnetic moments with synchotron radiation (APS at Argonne)

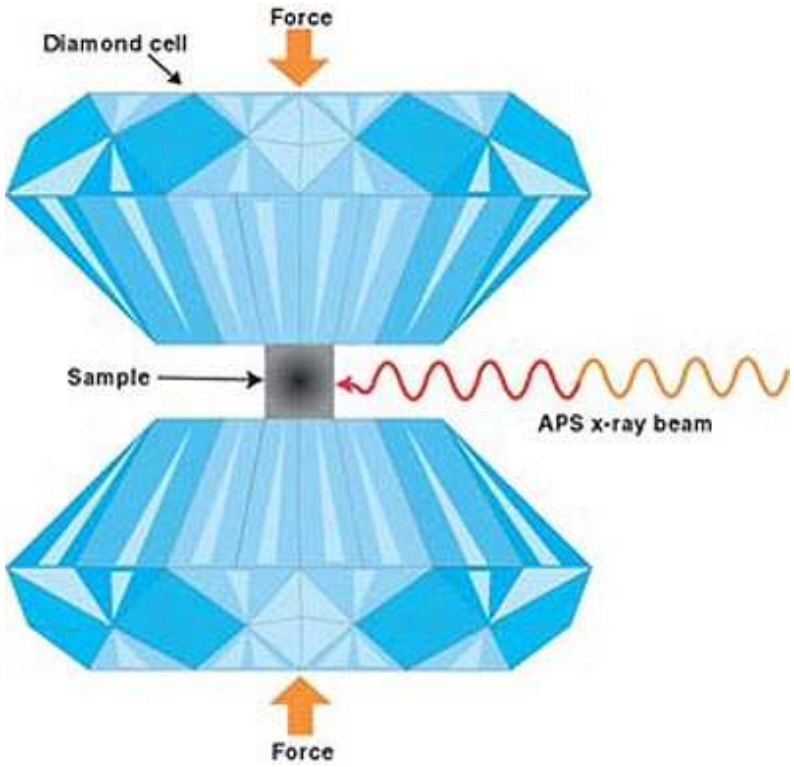

Cuprates

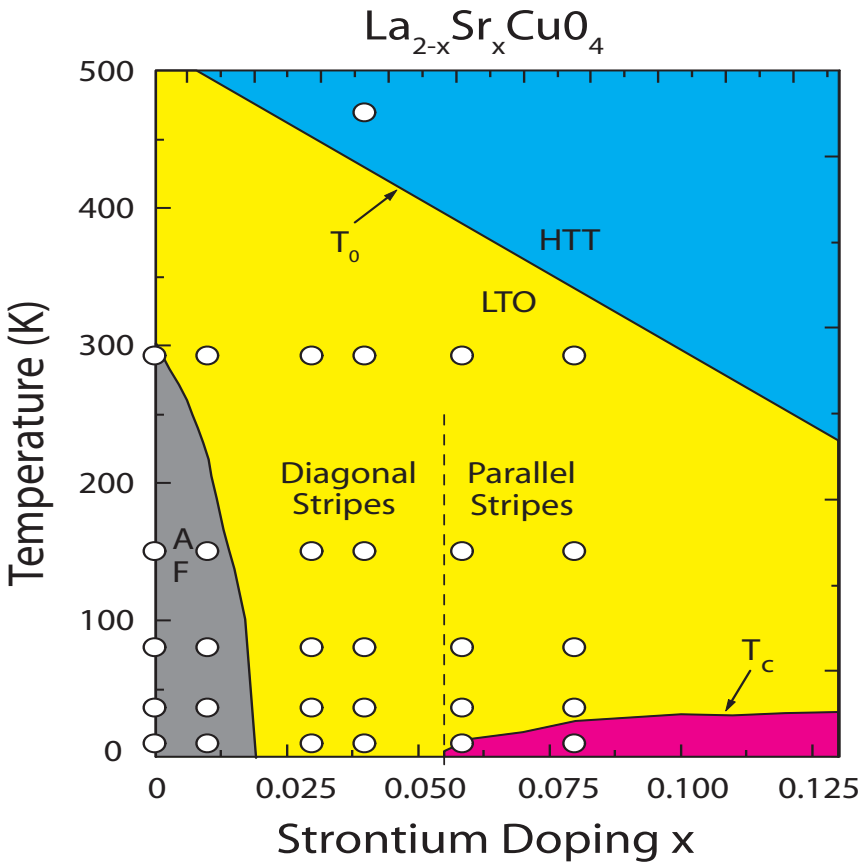

More complex phenomena, eg:

- Stripes (charge/spin inhomogeneities)
- d-wave superconductivity ???

Additional Degrees of freedom:

- Phonons
- Disorder

2. The Hubbard Hamiltonian

$$\hat{H} = -t \sum_{\langle \mathbf{ij} \rangle \sigma} (c^{\dagger}_{\mathbf{i}\sigma} c_{\mathbf{j}\sigma} + c^{\dagger}_{\mathbf{j}\sigma} c_{\mathbf{i}\sigma}) + U \sum_{\mathbf{i}} (n_{\mathbf{i}\uparrow} - \frac{1}{2})(n_{\mathbf{i}\downarrow} - \frac{1}{2}) - \mu \sum_{\mathbf{i}\sigma} (n_{\mathbf{i}\sigma} + n_{\mathbf{i}\sigma})$$

- $c^{\dagger}_{\mathbf{i}\sigma}$ ($c_{\mathbf{i}\sigma}$) are fermion creation(destruction) operators, site $\mathbf{i}$, spin $\sigma = \uparrow, \downarrow$.
- Kinetic energy t describes hopping between near-neighbor sites $\langle \mathbf{ij} \rangle$.
- Chemical potential μ controls filling.
- Describes qualitative "strong correlation" physics of many-electron materials

  Transition metal monoxides, cuprate superconductors, ...

  On-site repulsion U sufficiently large $\rightarrow$ Mott Insulator

  Exchange interaction $J \propto t^2/U \rightarrow$ Antiferromagnetism

  Stripes and other charge/spin inhomogeneities.

  d-wave superconductivity ???

Mott Insulators and Antiferromagnetism: Qualitative Pictures

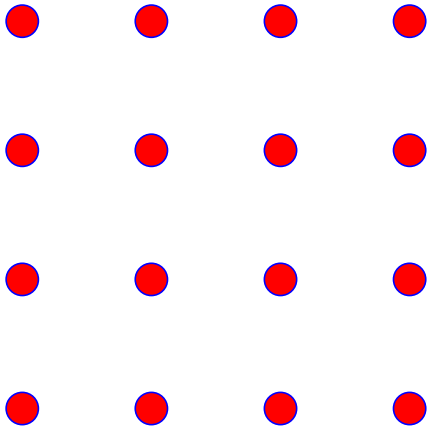

Consider a lattice of sites with
"commensurate filling":
The average number of electrons
is one per site.

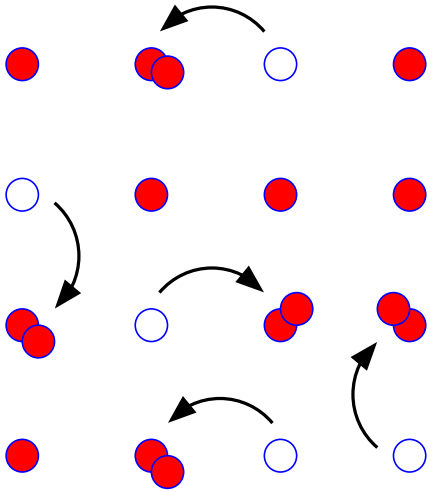

"quantum fluctuations" (kinetic energy t)
and thermal fluctuations T, both favor
electrons moving around lattice.
Metal: odd number (one) particle per cell/site.

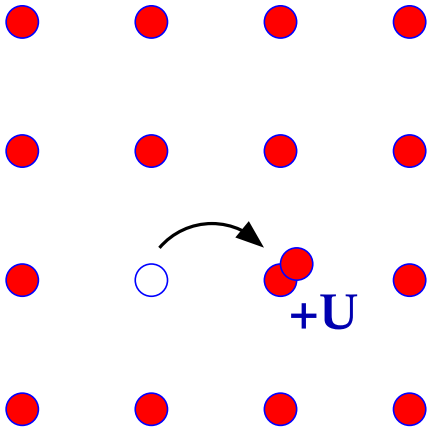

But what if there were a large repulsive interaction U between electrons on the same site?

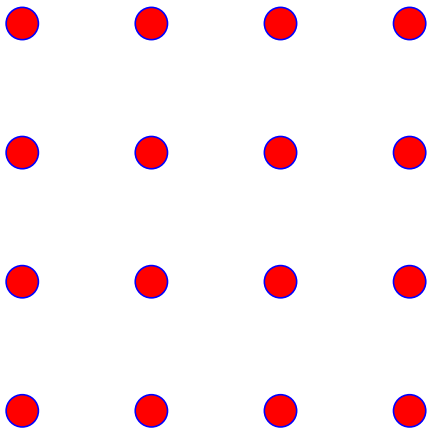

A Mott Insulator forms.

Despite half-filling!!

Basic physics of parent compounds of cuprate superconductors!

Two ways to destroy Mott Insulator:

* Decrease U/t: By applying pressure (MnO)
* Shift $\langle n \rangle \neq 1$: Dope chemically (cuprate superconductors)

What is optimal spin arrangement?

Hopping of neighboring parallel spins forbidden by Pauli.

Antiparallel arrangement lower in second order perturbation theory.

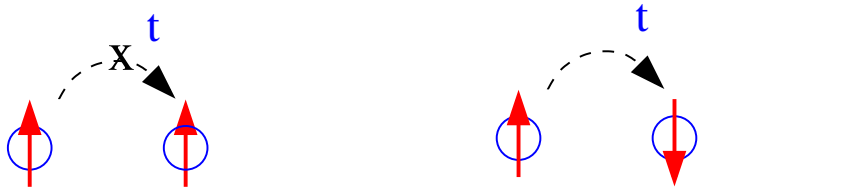

$\Delta E^{(2)} = 0$ $\qquad$ $\Delta E^{(2)} \propto -t^2/U = -J$

Mott insulating behavior and antiferromagnetism go hand-in-hand.
Qualitative picture of cuprate physics before doping.

Still do not fully understand why cuprates superconduct after doping.

3. Classical Monte Carlo

Why review?

Quantum MC in d spatial dimensions $\Rightarrow$ Classical MC in $d+1$ dimensions.

Feynman's path integral formulation of Quantum Mechanics:

Additional dimension is 'imaginary time' $\tau \in (0, \beta = 1/T)$.

Goal of Monte Carlo:

Generate configurations of degrees of freedom $\{X_j\}$ with probability $p\big(\{X_j\}\big)$

Classical statistical mechanics: $p\big(\{X_j\}\big) = \mathcal{Z}^{-1} e^{-E(\{X_j\})/k_{\rm B}T}$

Monte Carlo $\Leftrightarrow$ laboratory experiment

Computer generates $\{X_j\}$ $\Leftrightarrow$ Nature generates $\{X_j\}$

Very close analogies:

- Starting from sequence of configurations: Make measurements.
- Wait for sample to equilibrate before taking data
- More measurements $\rightarrow$ smaller error bars
- Closely spaced measurements might not be independent (correlation time).

How does one accomplish this? **And is it rigorous?**

Fundamental object in Monte Carlo:

Transition rule $\mathcal{T}_{ji}$: configuration $X_i \to X_j$.

Stochastic matrix: $\mathcal{T}_{ji} \geq 0$ $\sum_j \mathcal{T}_{ji} = 1$

Eigenvalues $|\lambda| \leq 1$.

$$\sum_i \mathcal{T}_{ji} v_i = \lambda v_j$$

$$\sum_i \mathcal{T}_{ji} |v_i| \geq \lambda |v_j| \qquad (\mathcal{T}_{ji} \geq 0 \text{ and triangle inequality})$$

$$\sum_i |v_i| \geq \lambda \sum_j |v_j| \qquad \left(\sum_j \mathcal{T}_{ji} = 1 \right)$$

Eigenvalues : $|\lambda| \leq \mathbf{1}$

Vector $v_i = 1$ obeys: $\sum_j v_j \mathcal{T}_{ji} = v_i$

So $\mathcal{T}$ has eigenvalue $\lambda = 1$.

Note: $v_i = 1$ is a left eigenvector of $\mathcal{T}$.

Left/Right eigenvalues are the same.

Left/Right eigenvectors can be different (if matrix not symmetric).

Construct $\mathcal{T}$ to obey detailed balance: $\mathcal{T}_{ji}\ p_i = \mathcal{T}_{ij}\ p_j$

p_i is (right) eigenvector of $\mathcal{T}$ with eigenvalue $\lambda = 1$.

$$\sum_i \mathcal{T}_{ji}\, p_i = \sum_i \mathcal{T}_{ij}\, p_j = p_j \sum_i \mathcal{T}_{ij} = p_j$$

Final point: Applying matrix repeatedly to $\vec{v} \Rightarrow$ eigenvector $\hat{e}_i$ of largest eigenvalue.

$$\mathcal{M}^L \vec{v} = \mathcal{M}^L \sum_i v_i\, \hat{e}_i = \sum_i v_i \lambda_i^L\, \hat{e}_i = \lambda_{\max}^L \sum_i v_i \Big(\frac{\lambda_i}{\lambda_{\max}}\Big)^L \hat{e}_i \Rightarrow \hat{e}_{\max}$$

Summary of rigorous foundation of (classical) Monte Carlo:

- Detailed balance: p is eigenvector of $\mathcal{T}$ of eigenvalue $\lambda = 1$
- $\mathcal{T}$ is stochastic: $|\lambda| \leq 1$
- $\mathcal{T}^P$ projects out eigenvector of largest eigenvalue.

Detailed balance can be implemented in several ways

- Metropolis algorithm: $\mathcal{T}_{ji} = \min\ (p_j/p_i, 1)$
- Heat bath algorithm: $\mathcal{T}_{ji} = p_j/(p_i + p_j) = (p_j/p_i)\ /\ \big(1 + (p_j/p_i)\big)$

Ising Model $E = -J \sum_{\langle ij \rangle} S_i S_j \qquad S_i = \pm 1$

Order parameter $M = \langle \sum_i S_i \rangle$ magnetization

Energy E favors parallel spin configurations:

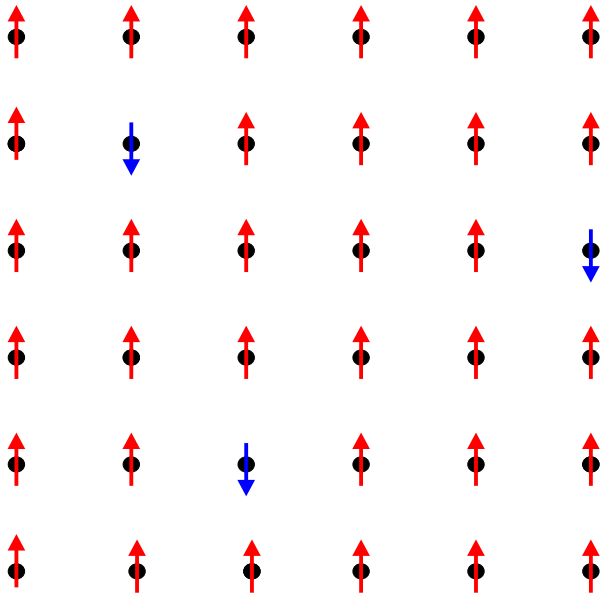

$M \neq 0$

Entropy S favors random spin configurations:

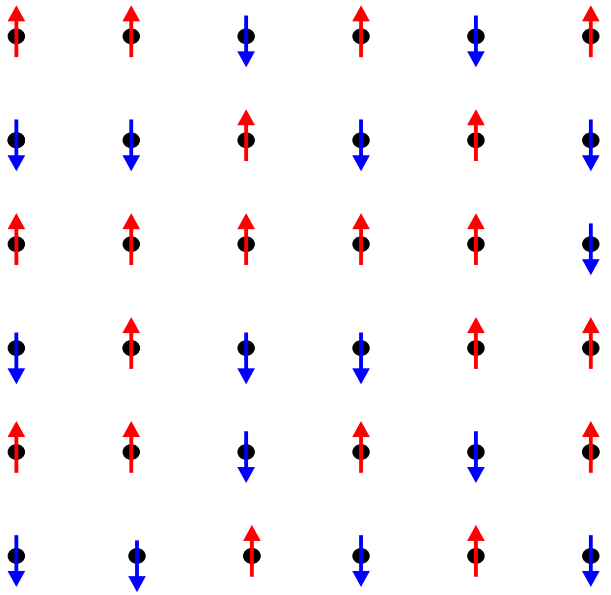

$M = 0$

Minimize Free Energy $F = E - TS$

Temperature T controls whether E or S wins.

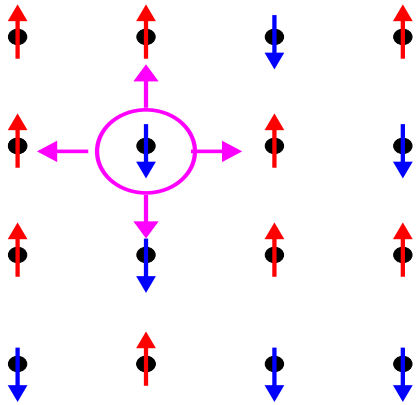

Select a spin. $\mathcal{T}_{ij}$ flips the spin.

Compute $\Delta E = -4J$. Local Calculation!

$p_j/p_i = e^{-\Delta E/k_{\rm B}T}$. No need for Z!

Repeat: Apply $\mathcal{T}_{ij}$ many times.

Results: Magnetic susceptibility

$\chi = \frac{1}{T}(\,\langle M^2\rangle - \langle M\rangle^2\,)$

Expense: ΔE is local

$\#(\text{ops}) = A\,N \quad A \sim 10$

$\sim 10^4$ for $N = 32 \times 32$ lattice.

Laptop CPU: 10^9 ops/sec

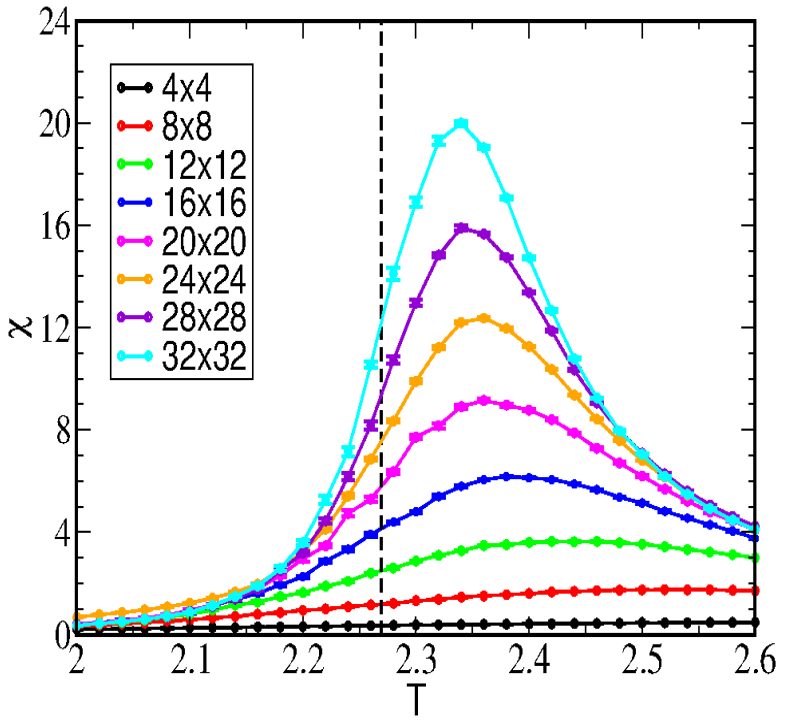

4. World Line Quantum Monte Carlo (Bosonic atoms)

QMC: Map Quantum problem in d spatial dimensions

$\rightarrow$ classical problem in $d+1$ dimensions via path integral.

WLQMC for anharmonic quantum oscillator in detail,

Sketch methodology for fermion and boson Hubbard models.

$$Z = \mathrm{Tr}\ e^{-\beta \hat{H}} \qquad\qquad \hat{H} = \frac{\hat{P}^2}{2m} + \frac{1}{2} m\omega^2 \hat{X}^2 + \frac{1}{4}\lambda \hat{X}^4.$$

Trotter Approximation: If $\hat{A}$ and $\hat{B}$ do not commute

$$e^{-\Delta\tau(\hat{A}+\hat{B})} \sim e^{-\Delta\tau\hat{A}} e^{-\Delta\tau\hat{B}} + o(\Delta\tau^2)$$

Need $\Delta\tau$ small, so discretize imaginary time: $\beta = L\,\Delta\tau$.

$$Z_{\mathrm{tr}} = \mathrm{Tr}\ \left[e^{-\Delta\tau \frac{\hat{P}^2}{2m}} e^{-\Delta\tau m\omega^2 \frac{\hat{X}^2}{2} - \Delta\tau\lambda\frac{\hat{X}^4}{4}} \right]^L$$

Controlled approximation: $\Delta\tau \rightarrow 0$: reduce error to any desired accuracy.

Express trace as a sum over a complete set of position eigenstates.

$$Z_{\rm tr} = \int dx_1 \, \langle x_1 | \, \left[e^{-\Delta\tau \frac{\hat{P}^2}{2m}} \, e^{-\Delta\tau m\omega^2 \frac{\hat{X}^2}{2} - \Delta\tau\lambda \frac{\hat{X}^4}{4}} \right]^L \, | x_1 \rangle,$$

Insert complete sets of eigenstates between each incremental time evolution operator,

$$\begin{aligned} Z_{\rm tr} = \int dx_1 \, dx_2 \, dx_3 \cdots dx_L \, & \langle x_1 | e^{-\Delta\tau \frac{\hat{P}^2}{2m}} e^{-\Delta\tau m\omega^2 \frac{\hat{X}^2}{2} - \Delta\tau\lambda \frac{\hat{X}^4}{4}} | x_2 \rangle \\ & \langle x_2 | e^{-\Delta\tau \frac{\hat{P}^2}{2m}} e^{-\Delta\tau m\omega^2 \frac{\hat{X}^2}{2} - \Delta\tau\lambda \frac{\hat{X}^4}{4}} | x_3 \rangle \cdots \\ & \langle x_L | e^{-\Delta\tau \frac{\hat{P}^2}{2m}} e^{-\Delta\tau m\omega^2 \frac{\hat{X}^2}{2} - \Delta\tau\lambda \frac{\hat{X}^4}{4}} | x_1 \rangle. \\ = \int dx_1 \, dx_2 \, dx_3 \cdots dx_L \, & e^{-\frac{1}{2} m\omega^2 \Delta\tau \sum_l x_l^2 - \frac{1}{4}\lambda\Delta\tau \sum_l x_l^4} \\ & \langle x_1 | e^{-\Delta\tau \frac{\hat{P}^2}{2m}} | x_2 \rangle \langle x_2 | e^{-\Delta\tau \frac{\hat{P}^2}{2m}} | x_3 \rangle \cdots \langle x_L | e^{-\Delta\tau \frac{\hat{P}^2}{2m}} | x_1 \rangle. \end{aligned}$$

Position operators $\hat{X}$ $\rightarrow$ c-numbers (eigenvalues).

Remaining (momentum operator) matrix elements can be evaluated:

$$\begin{aligned} \langle x_l | e^{-\Delta\tau \frac{\hat{P}^2}{2m}} | x_{l+1} \rangle &= \int dp \, \langle x_l | e^{-\Delta\tau \frac{\hat{P}^2}{2m}} | p \rangle \langle p | x_{l+1} \rangle \\ = \int dp \, e^{-\Delta\tau p^2/2m} e^{ip(x_l - x_{l+1})} &= \sqrt{\frac{2m\pi}{\Delta\tau}} e^{-\frac{1}{2} m\Delta\tau [(x_l - x_{l+1})/\Delta\tau]^2}. \end{aligned}$$

Z is now expressed entirely as a multi-dimensional integral over *classical* variables,

$$Z_{\rm tr} = \int dx_1\, dx_2 \cdots dx_L\; e^{-\Delta\tau S_{\rm cl}}$$

$$S_{\rm cl}\big(\{x_l\}\big) = \frac{1}{2}m\omega^2 \sum_l x_l^2 + \frac{1}{4}\lambda \sum_l x_l^4 + \frac{1}{2}m \sum_l \Big(\frac{x_l - x_{l+1}}{\Delta\tau}\Big)^2,$$

Original quantum degree of freedom $\hat{X} \Rightarrow x_l$

Additional Imaginary time index: path described by classical variables x_l.

Trotter Errors ($\Delta\tau = 0.25, m = \omega = 1, \lambda = 0$):

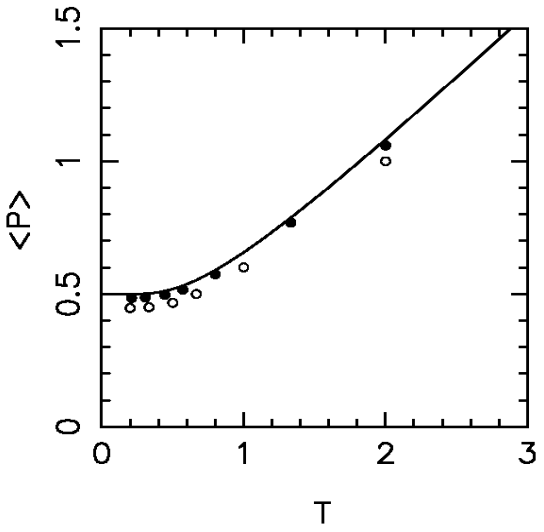

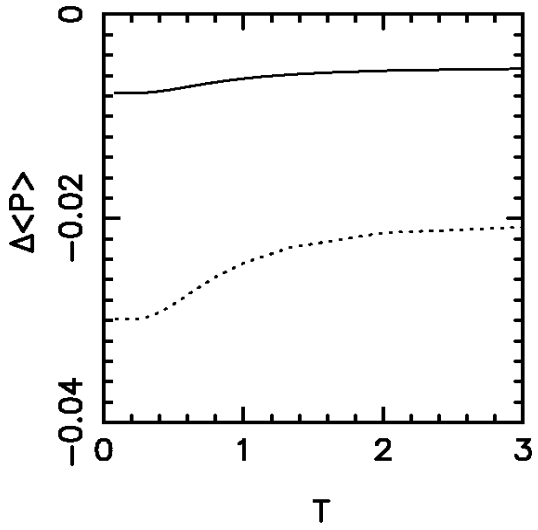

Major challenge for world line QMC:

Long autocorrelation times

Origin: separation in imaginary time scales

"Floppy springs": PE $\sim \frac{1}{2}\Delta\tau\, m\,\omega^2\, x_l^2$

"Tight springs": KE $\sim \frac{1}{2}\Delta\tau \frac{\left(x_{l+1}-x_l\right)^2}{\Delta\tau^2}$

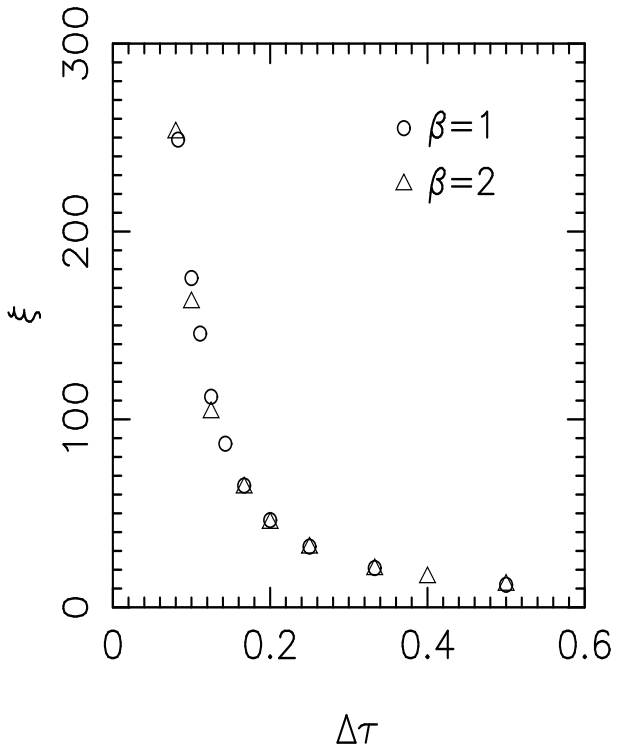

For bosons and quantum spins, this problem is solved!

Stochastic series expansion, loop, and worm algorithms

Remains a major computational bottleneck for interacting electron-phonon models.

World-Line Quantum Monte Carlo Simulations: (boson, fermion) Hubbard models

As for QHO, discretize $\beta = L\Delta\tau$ and subdivide $\hat{H} = \hat{H}_a + \hat{H}_b$

$$Z = \mathrm{Tr}\, e^{-\beta\hat{H}} = \mathrm{Tr}\left[e^{-\Delta\tau\hat{H}}\right]^L \sim \mathrm{Tr}\left[e^{-\Delta\tau\hat{H}_a}\, e^{-\Delta\tau\hat{H}_b}\right]^L$$

Insert complete sets of occupation number states

$$Z = \sum_{n_l} \langle n_0|e^{-\Delta\tau\hat{H}_a}|n_1\rangle\langle n_1|e^{-\Delta\tau\hat{H}_b}|n_2\rangle\langle n_2|e^{-\Delta\tau\hat{H}_a}|n_3\rangle\langle n_3|e^{-\Delta\tau\hat{H}_b}|n_4\rangle$$
$$\cdots\langle n_{2L-2}|e^{-\Delta\tau H_a}|n_{2L-1}\rangle\langle n_{2L-1}|e^{-\Delta\tau H_b}|n_0\rangle$$

Imaginary time l explicit; spatial index implicit: $|n_l\rangle \equiv |n_{1l}\ n_{2l}\ n_{3l}\cdots\rangle$.

Central to WLQMC: be able to evaluate matrix elements of $e^{-\Delta\tau H_\alpha}$

Very useful trick: "Checkerboard Decomposition"

Divide Hamiltonian into pieces each comprised of independent two site problems

$$\hat{H}_a = -J\sum_{i\in\,\mathrm{odd}}(\hat{b}_i^\dagger\hat{b}_{i+1} + \hat{b}_{i+1}^\dagger\hat{b}_i) + \frac{U}{2}\sum_i \hat{n}_i^2 - \frac{\mu}{2}\sum_i \hat{n}_i$$
$$\hat{H}_b = -J\sum_{i\in\,\mathrm{even}}(b_i^\dagger b_{i+1} + b_{i+1}^\dagger b_i) + \frac{U}{2}\sum_i \hat{n}_i^2 - \frac{\mu}{2}\sum_i \hat{n}_i$$

For $\hat{H}_a$:

$$\langle n_{1l}\, n_{2l}\, n_{3l}\, n_{4l} \cdots | e^{J\Delta\tau(\hat{b}_1^\dagger \hat{b}_2 + \hat{b}_2^\dagger \hat{b}_1) - \frac{U\Delta\tau}{2}(\hat{n}_1^2+\hat{n}_2^2) - \frac{\mu\Delta\tau}{2}(\hat{n}_1+\hat{n}_2)}$$
$$e^{J\Delta\tau(\hat{b}_3^\dagger \hat{b}_4 + \hat{b}_4^\dagger \hat{b}_3) - \frac{U\Delta\tau}{2}(\hat{n}_3^2+\hat{n}_4^2) - \frac{\mu\Delta\tau}{2}(\hat{n}_3+\hat{n}_4)} \cdots | n_{1l+1}\, n_{2l+1}\, n_{3l+1}\, n_{4l+1} \cdots \rangle$$
$$= \langle n_{1l}\, n_{2l} | e^{J\Delta\tau(\hat{b}_1^\dagger \hat{b}_2 + \hat{b}_2^\dagger \hat{b}_1) - \frac{U\Delta\tau}{2}(\hat{n}_1^2+\hat{n}_2^2) - \frac{\mu\Delta\tau}{2}(\hat{n}_1+\hat{n}_2)} | n_{1l+1}\, n_{2l+1} \rangle$$
$$\langle n_{3l}\, n_{4l} | e^{J\Delta\tau(\hat{b}_3^\dagger \hat{b}_4 + \hat{b}_4^\dagger \hat{b}_3) - \frac{U\Delta\tau}{2}(\hat{n}_3^2+\hat{n}_4^2) - \frac{\mu\Delta\tau}{2}(\hat{n}_3+\hat{n}_4)} | n_{3l+1}\, n_{4l+1} \rangle \cdots$$

Note the factorization into independent two-site problems.

Need table of two site problem matrix elements.

For fermions and hard-core bosons:

$$\langle 1\,0 | e^{J\Delta\tau(\hat{b}_1^\dagger \hat{b}_2 + \hat{b}_2^\dagger \hat{b}_1) - \frac{U\Delta\tau}{2}(\hat{n}_1^2+\hat{n}_2^2) - \frac{\mu\Delta\tau}{2}(\hat{n}_1+\hat{n}_2)} | 1\,0 \rangle = \cosh(J\Delta\tau)\, e^{-\frac{U\Delta\tau}{2} - \frac{\mu\Delta\tau}{2}}$$
$$\langle 1\,0 | e^{J\Delta\tau(\hat{b}_1^\dagger \hat{b}_2 + \hat{b}_2^\dagger \hat{b}_1) - \frac{U\Delta\tau}{2}(\hat{n}_1^2+\hat{n}_2^2) - \frac{\mu\Delta\tau}{2}(\hat{n}_1+\hat{n}_2)} | 0\,1 \rangle = \sinh(J\Delta\tau)\, e^{-\frac{U\Delta\tau}{2} - \frac{\mu\Delta\tau}{2}}$$
$$\langle 1\,1 | e^{J\Delta\tau(\hat{b}_1^\dagger \hat{b}_2 + \hat{b}_2^\dagger \hat{b}_1) - \frac{U\Delta\tau}{2}(\hat{n}_1^2+\hat{n}_2^2) - \frac{\mu\Delta\tau}{2}(\hat{n}_1+\hat{n}_2)} | 1\,1 \rangle = e^{-2U\Delta\tau - \mu\Delta\tau} \quad \text{etc} \cdots$$

Worldline probability: matrix element product across space-time lattice.

Not of form $p \sim e^{-E/k_{\rm B}T}$, but monte carlo works for any p!

State of system represented by occupation number paths $n(i, \tau)$

Paths sampled stochastically. Shaded squares indicate where Ha, H_b contribute.

Propose moves of world lines. Evaluate (local!) change to matrix element product.

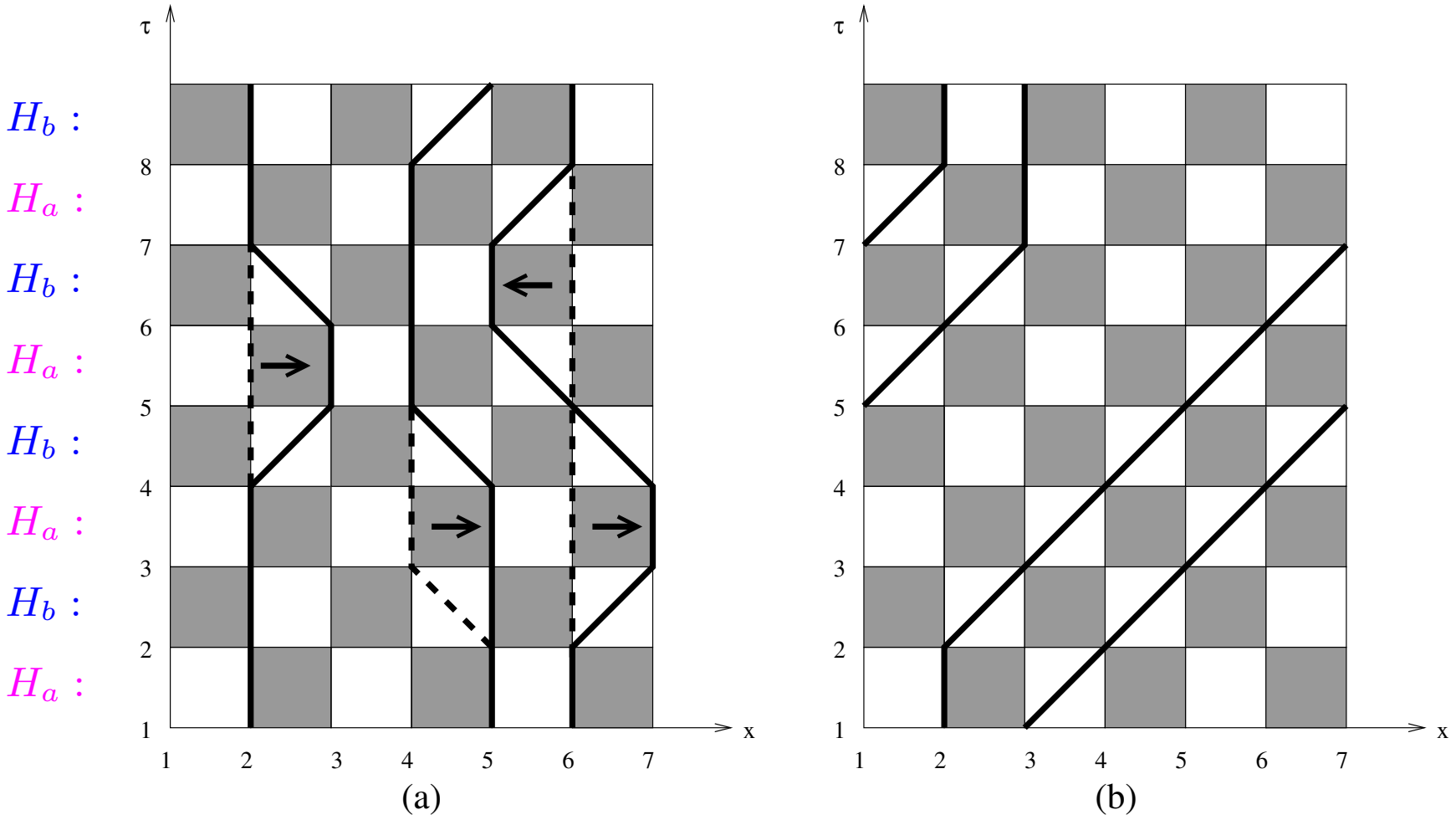

Zero Winding

Non-Zero winding

Key features of (original) World Line QMC:

- Linear scaling in particle number (system size).
- (Very) Long autocorrelation times.
- Cannot measure Green's function $G_{ij}^{\sigma} = \langle c_{i\sigma}^{\dagger} c_{j\sigma} \rangle$ (would break world lines).
- Sign problem for fermions and frustrated quantum spins.

Advances:

- Continuous time algorithms eliminate β discretization. No Trotter errors.
- Loop and worm algorithms improve sampling.
  Autocorrelation times decrease by 3-4 orders of magnitude.
  Sample nonzero winding sectors.
- Extend measurements.
  Superfluid density ρ_s.
  Greens function ('worms' allow 'broken' world lines); $n(k)$.

Bottom line:

- Can simulate $10^4 - 10^6$ quantum bosons/spins.
- Very high precision on critical points, exponents.
- Address very subtle issues in nature of phase transitions.

- Sign problem remains for fermions.

Phase diagram

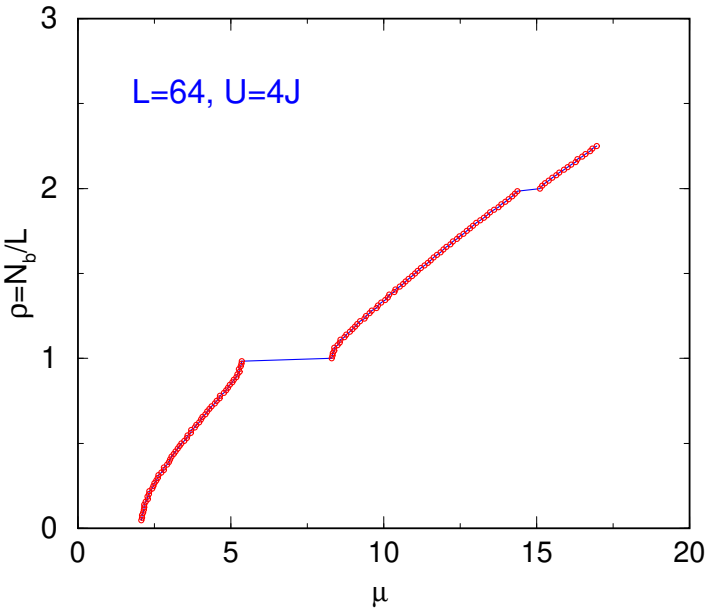

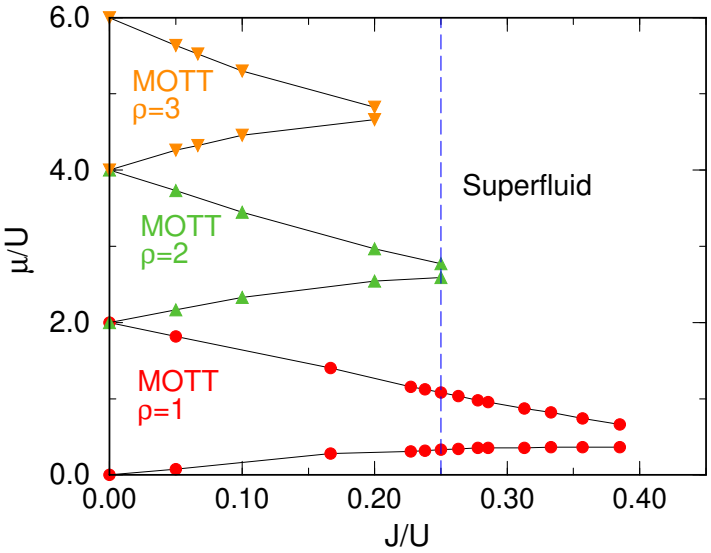

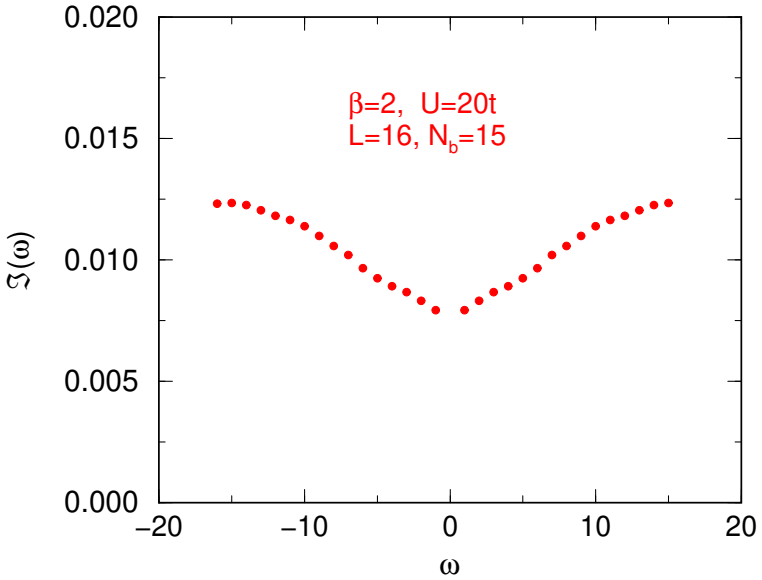

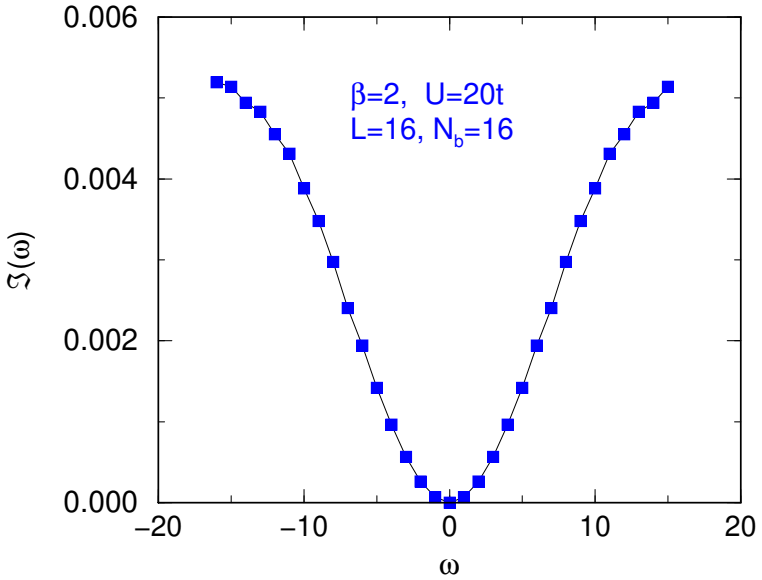

Cold Atoms: One dimensional trapped Boson Hubbard model

No globally incompressible Mott plateau in the trapped system! As a whole, the system is always compressible.

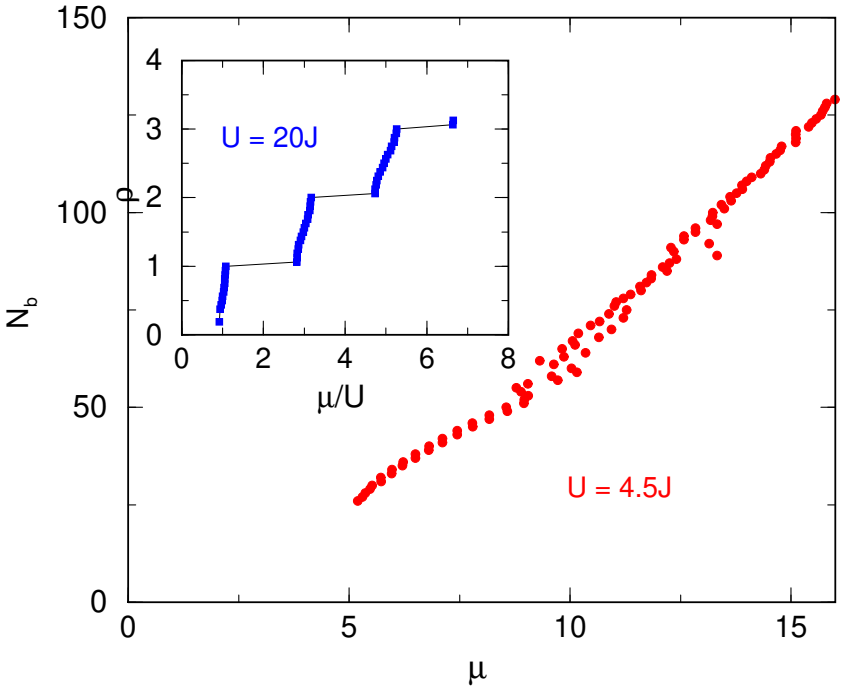

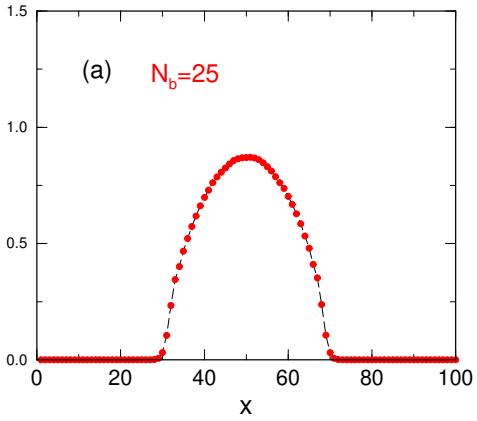

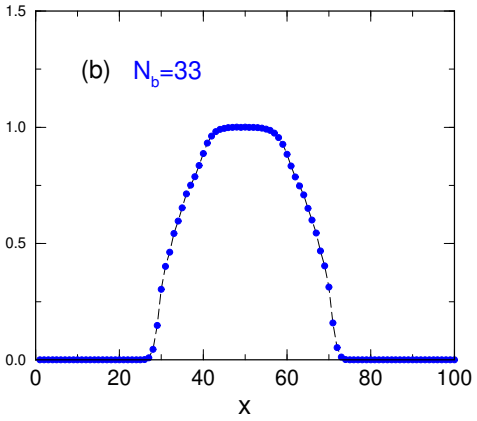

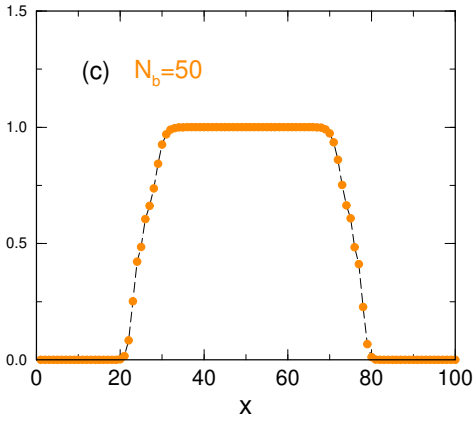

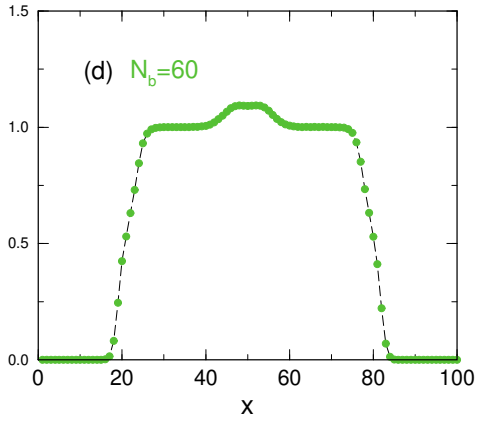

Two dimensional Bose Hubbard Hamiltonian with confining potential.

QMC density, number fluctuation, and compressibility profiles:

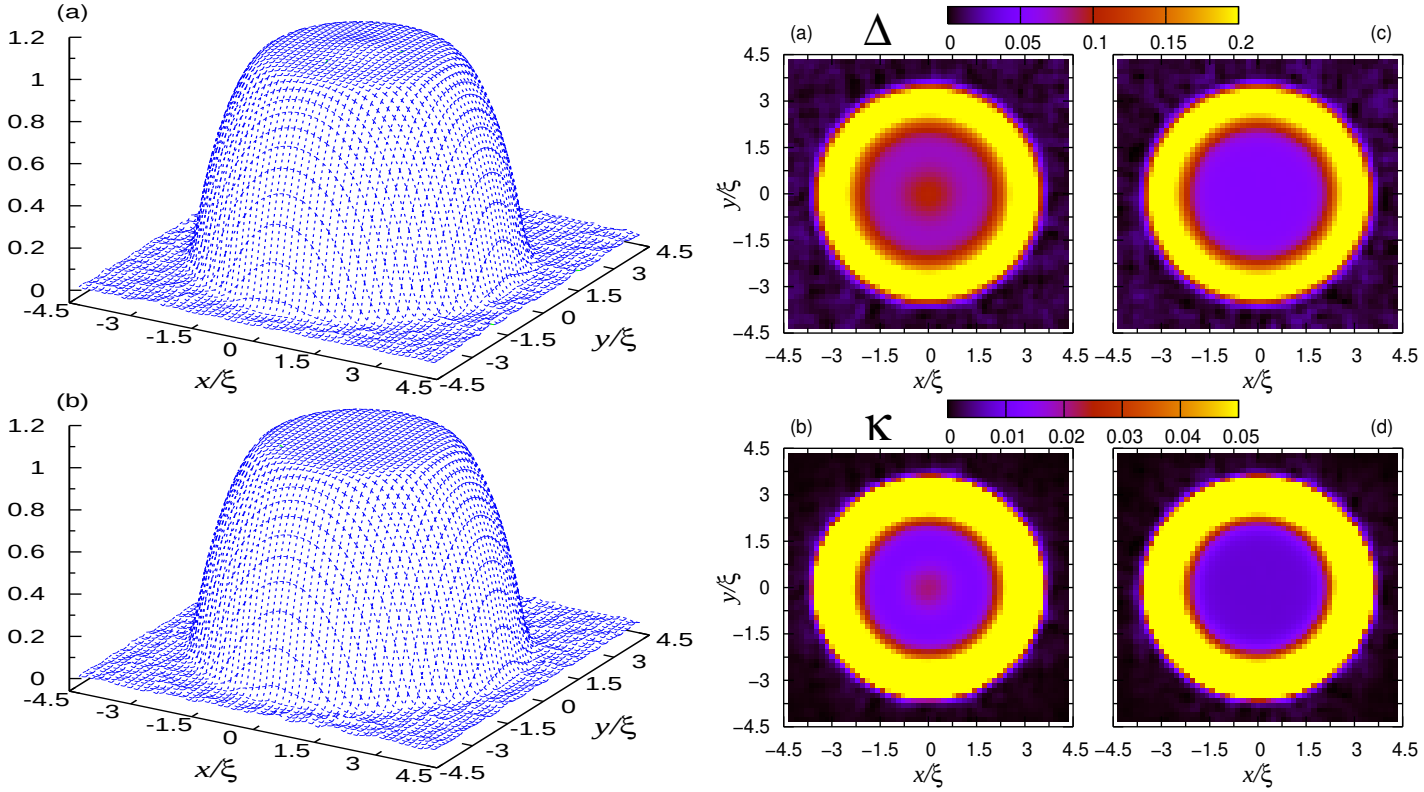

Top: $U/J = 17.5$ Bottom: $U/J = 18.5$ Uniform: $(U/J)_c = 16.7$

$N_b = 1200$, $V_{\rm trap}/J = 0.025$.

Despite extra energy scale (confining V), no more parameters than homogeneous case!

Curvature $V_{\rm trap}$ provides length scale $\xi = \sqrt{\frac{J}{V_{\rm trap}}}$

Plays same role as linear lattice size

"Characteristic Density" $\tilde{\rho} = N_b/\xi^d$

Can meaningfully compare systems with different $V_{\rm trap}$.

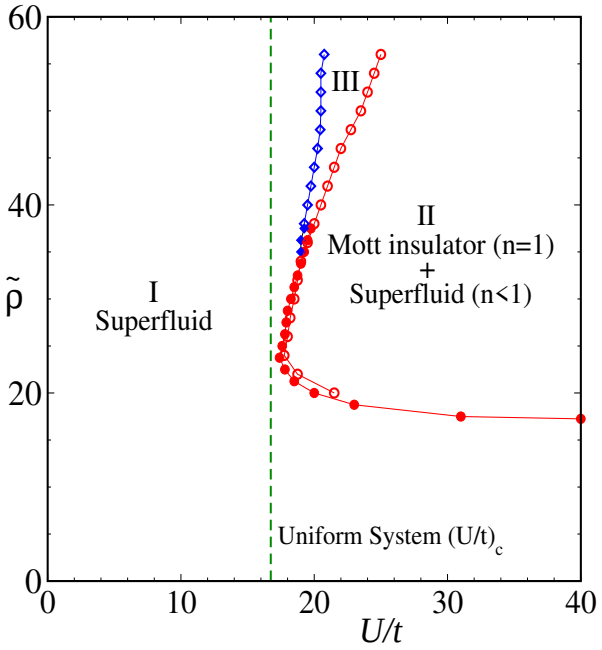

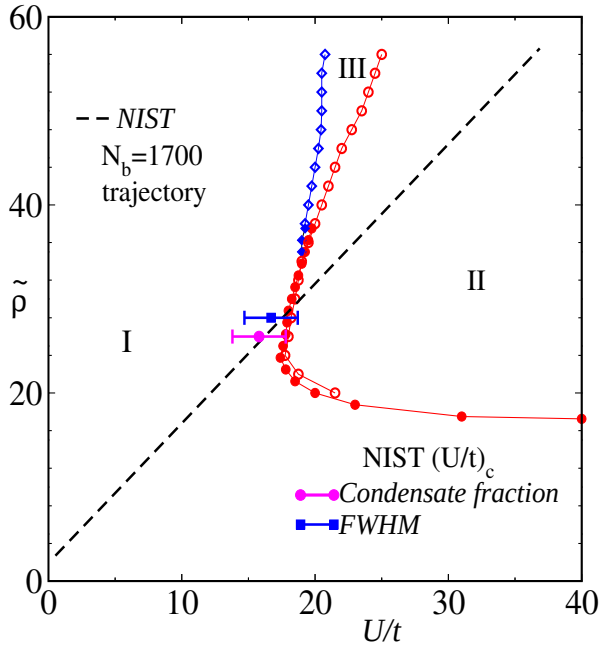

Right: Comparisons with experiments at NIST.

M. Rigol, G.G. Batrouni, V.G. Rousseau, and RTS, Phys. Rev. **A79**, 053605 (2009).

Visualizing the physics of spinless fermions (in $d = 1$):

Near neighbor repulsion V.

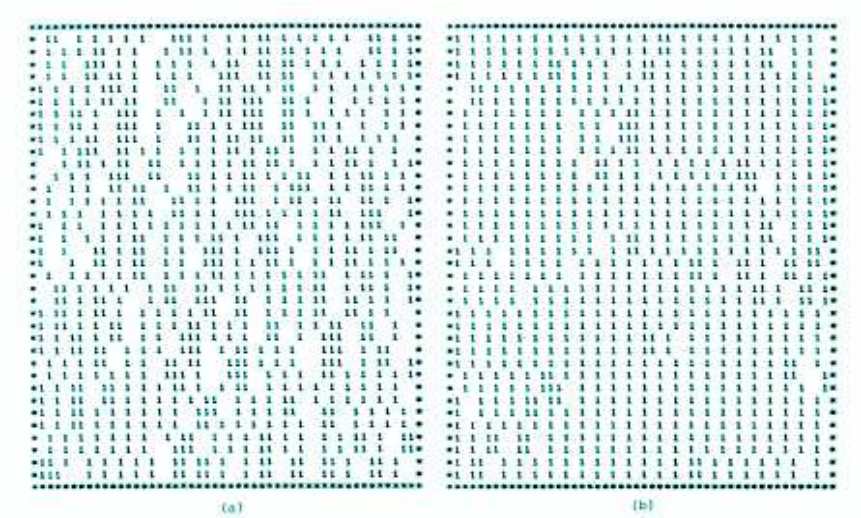

Charge density wave transition

Half-filled lattice

Left: $J = 1, V = 0$

Right: $J = 1, V = 3$

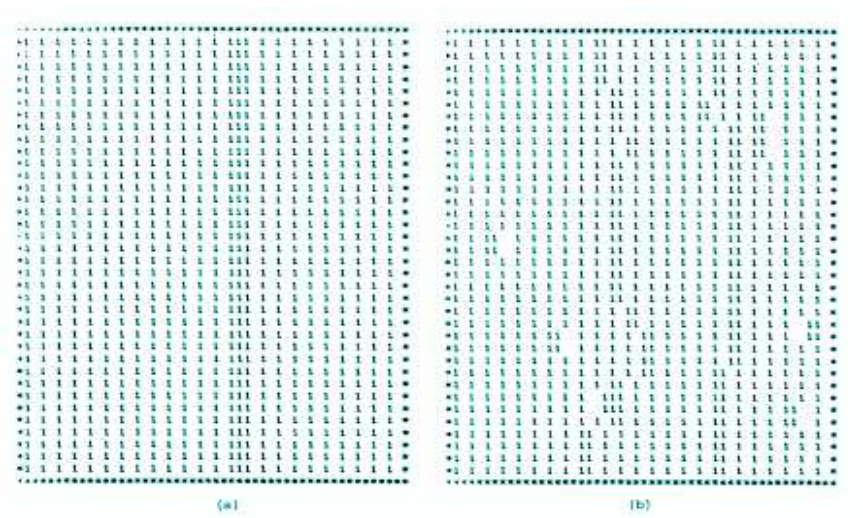

Soliton formation

Half-filled + 1 added particle

$J = 1, V = 4$

Left: Initial configuration

Right: After equilibration

Breaks into two charge-1/2 entities!

Visualizing the physics of spin-$\frac{1}{2}$ fermions:

On-site repulsion U (Hubbard Model)

Half-filled lattice J=1

+: spin up −: spin down #: doubly occupied

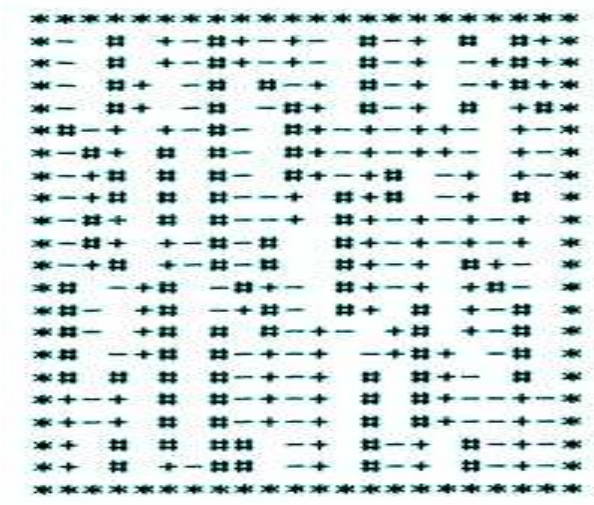

$U = 0$

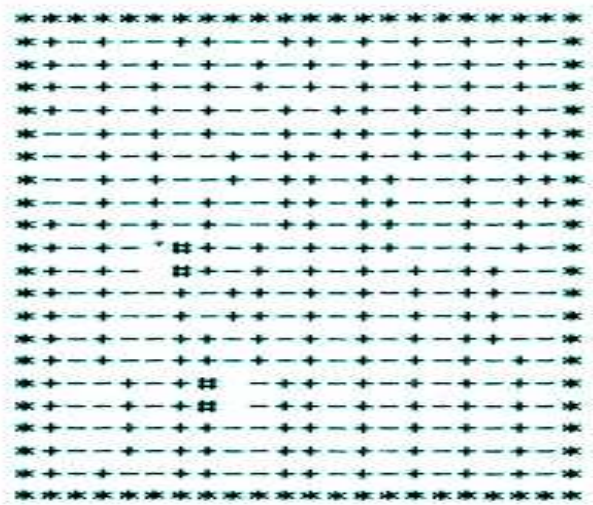

$U = 6$

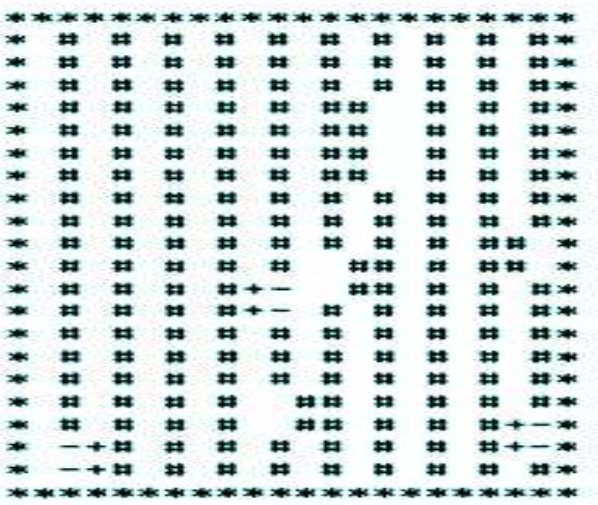

$U = -6, V = 0.4$

Center: Antiferromagnetic phase

Right: Charge density wave phase

5. Determinant Quantum Monte Carlo (Fermionic atoms)

DQMC formalism very similar to idenities of multidimensional Gaussian integrals.

Analogy provides intuitive feel for formulae of determinant QMC.

(Trivial) dimensional Gaussian integral:

$$\int_{-\infty}^{+\infty} dx\, e^{-ax^2} = \frac{\sqrt{\pi}}{a},$$

Generalization to many dimensions:

$$Z = \int_{-\infty}^{+\infty} \int_{-\infty}^{+\infty} \cdots \int_{-\infty}^{+\infty} dx_1 dx_2 \cdots dx_N \; e^{-\vec{x}\, A\, \vec{x}^{\,T}} = \frac{\pi^{n/2}}{\sqrt{\det A}}.$$

$\vec{x}$: N dimensional vector of numbers. A : symmetric N dimensional matrix.

Notation emphasizes this is partition function Z for $E = \vec{x} A \vec{x}^{\,T}$.

Integrand including factors of x_i.

$$\langle x_i x_j \rangle = Z^{-1} \int_{-\infty}^{+\infty} \int_{-\infty}^{+\infty} \cdots \int_{-\infty}^{+\infty} dx_1 dx_2 \ldots dx_N \; x_i x_j \; e^{-\vec{x}\, A\, \vec{x}^{\,T}} = \frac{1}{2}[A^{-1}]_{ij}$$

Notation $\langle x_i x_j \rangle$ emphasizes statistical mechanical interpretation.

Our goal in DQMC: compute operator expectation values!

$$\begin{aligned} \langle \hat{A} \rangle &= Z^{-1} \text{ Tr } [\hat{A} e^{-\beta \hat{H}}] \\ Z &= \text{Tr } [e^{-\beta \hat{H}}] \end{aligned}$$

Hubbard Hamiltonian

$$\hat{H} = -t \sum_{\langle \mathbf{ij} \rangle \sigma} (c^{\dagger}_{\mathbf{i}\sigma} c_{\mathbf{j}\sigma} + c^{\dagger}_{\mathbf{j}\sigma} c_{\mathbf{i}\sigma}) + U \sum_{\mathbf{i}} (n_{\mathbf{i}\uparrow} - \frac{1}{2})(n_{\mathbf{i}\downarrow} - \frac{1}{2}) - \mu \sum_{\mathbf{i}\sigma} (n_{\mathbf{i}\sigma} + n_{\mathbf{i}\sigma})$$

Similar to WLQMC, mapping to $d+1$ using path integral.

- Inverse Temperature discretized: $\beta = L\Delta\tau$

$$Z = \text{Tr } [e^{-\beta \hat{H}}] = \text{Tr } [e^{-\Delta\tau \hat{H}}]^L$$

- Suzuki-Trotter Approximation

$$e^{-\Delta\tau \hat{H}} \approx e^{-\Delta\tau \hat{K}} e^{-\Delta\tau \hat{P}}$$

Extrapolation to $\Delta\tau = 0$.

- (Discrete) Hubbard-Stratonovich Field (Hirsch) decouples interaction:

$$e^{-\Delta\tau U(\hat{n}_{\mathbf{i}\uparrow}-\frac{1}{2})(\hat{n}_{\mathbf{i}\downarrow}-\frac{1}{2})} = \frac{1}{2}e^{-U\Delta\tau/4}\sum_{S_{\mathbf{i}\tau}} e^{\Delta\tau\lambda S_{\mathbf{i}\tau}(\hat{n}_{\mathbf{i}\uparrow}-\hat{n}_{\mathbf{i}\downarrow})} = e^{-\Delta\tau\hat{\mathbb{C}}_{\mathbf{i}}(\tau)}$$

where $\cosh(\Delta\tau\lambda) = e^{U\Delta\tau/2}$.

- Quadratic Form in fermion operators: Do trace analytically

$$\begin{aligned} Z &= \sum_{\{S_{\mathbf{i}\tau}\}} \mathrm{Tr}\left[e^{-\Delta\tau\hat{\mathcal{K}}}e^{-\Delta\tau\hat{\mathcal{V}}(1)}e^{-\Delta\tau\hat{\mathcal{K}}}e^{-\Delta\tau\hat{\mathcal{V}}(2)}e^{-\Delta\tau\hat{\mathcal{K}}}\ldots e^{-\Delta\tau\hat{\mathcal{V}}(L)}\right] \\ &= \sum_{\{S_{\mathbf{i}\tau}\}} \det M_\uparrow(\{S_{\mathbf{i}\tau}\})\,\det M_\downarrow(\{S_{\mathbf{i}\tau}\}) \end{aligned}$$

$\hat{\mathcal{K}}$ and $\hat{\mathcal{V}}$ are operators.

Nevertheless, structural similarities to mulidimensional Gaussian integrals.

M_σ are matrices of numbers. $\dim(M_\sigma)$ is number of spatial sites.

$$M_\sigma = I + B_{1\sigma}\,B_{2\sigma}\,B_{3\sigma}\cdots B_{L\sigma} \qquad\qquad B_l = e^{k}e^{v_{l\sigma}}$$

k and v are matrices of numbers which build up M_σ.

Detailed structure of the M_σ matrices:

$$M_\sigma = I + B_{1\sigma}\, B_{2\sigma}\, B_{3\sigma} \cdots B_{L\sigma} \qquad\qquad B_l = e^k e^{v_{l\sigma}}$$

Kinetic energy matrix (in $d = 1$):

$$k = \Delta\tau \begin{bmatrix} -\mu & -t & 0 & 0 & \cdots \\ -t & -\mu & -t & 0 & \cdots \\ 0 & -t & -\mu & -t & \cdots \\ 0 & 0 & -t & -\mu & \cdots \\ \vdots & \vdots & \vdots & \vdots & \ddots \end{bmatrix}$$

Potential energy matrix:

$$v_{l\sigma} = \pm \begin{bmatrix} \lambda S_{1l} & 0 & 0 & 0 & \cdots \\ 0 & \lambda S_{2l} & 0 & 0 & \cdots \\ 0 & 0 & \lambda S_{2l} & 0 & \cdots \\ 0 & 0 & 0 & \lambda S_{2l} & \cdots \\ \vdots & \vdots & \vdots & \vdots & \ddots \end{bmatrix}$$

where $\pm$ for $\sigma = \uparrow, \downarrow$, and $\cosh(\Delta\tau\lambda) = e^{U\Delta\tau/2}$.

Checkerboard $k = k_a + k_b$ to speed computation of e^k.

- Sample HS field stochastically.

$$\begin{aligned} S_{\mathbf{i_0}\tau_0} &\rightarrow -S_{\mathbf{i_0}\tau_0} \\ \det M_\sigma(\{S_{\mathbf{i}\tau}\}) &\rightarrow \det M_\sigma(\{S_{\mathbf{i}\tau}\}') \end{aligned}$$

Computation of new determinant is o(N^3).
Most naive algorithm is order o$(N^4 L)$ since NL HS variables.
Local nature of change in HS field: evaluate ratio of determinants $o(N^2)$.

Algorithm is order $N^3 L$.
$N \sim \quad 10^2 - 10^3$ lattice sites/electrons (compare 10^6 quantum spins/bosons).
$L = \beta/\Delta\tau \sim$ a hundred imaginary time slices (low temperatures).

- Measurements (Gaussian integral analogy $\cdots$)

$$\langle \hat{c}_{\mathbf{i}\sigma} \hat{c}^\dagger_{\mathbf{j}\sigma} \rangle \leftrightarrow \langle [M_\sigma^{-1}]_{\mathbf{ij}} \rangle = \langle [G_\sigma]_{\mathbf{ij}} \rangle$$

- Sign Problem

At low temperature $\det M_\sigma$ can go negative.
CPU time grows exponentially.
No Sign Problem with special symmetry (half-filling $\rho = 1$) or $U < 0$.

Key features of (original) Determinant QMC:

- Algorithm is order $N^3 L$. (Computation of determinants.)
- $N \sim 10^2$ lattice sites (fermions).
  $L = \beta/\Delta\tau \sim 200$ (to reach low temperatures).
  Ground state projection methods (Sorella, S-W. Zhang)
- Sign Problem
  At low temperature $\det M_\sigma$ can go negative.
  However, typically occurs at $T \sim t/4$.
  Order of magnitude lower T than WLQMC!
  T cold enough to characterize short range spin/charge correlations.
  Special cases ($U > 0, \rho = 1$; or any $U < 0$, all ρ): sign $\det M_\uparrow, \det M_\downarrow$ same.
  Constrained Path Approaches (S-W. Zhang)

Advances:

- $N \sim 10^2 \rightarrow N \sim 10^3$ fermions (collaborate with CS researchers: D'Azevedo; Bai)
- Integration with Electronic Structure Codes via "dynamical mean field theory"
- Continuous time solvers for DMFT.
- Langevin updates of HS fields (linear scaling with N) Batrouni, Barros, Cohen-Stead

Prospect: Treat strongly correlated material rather than models.

Sign problem at generic fillings.

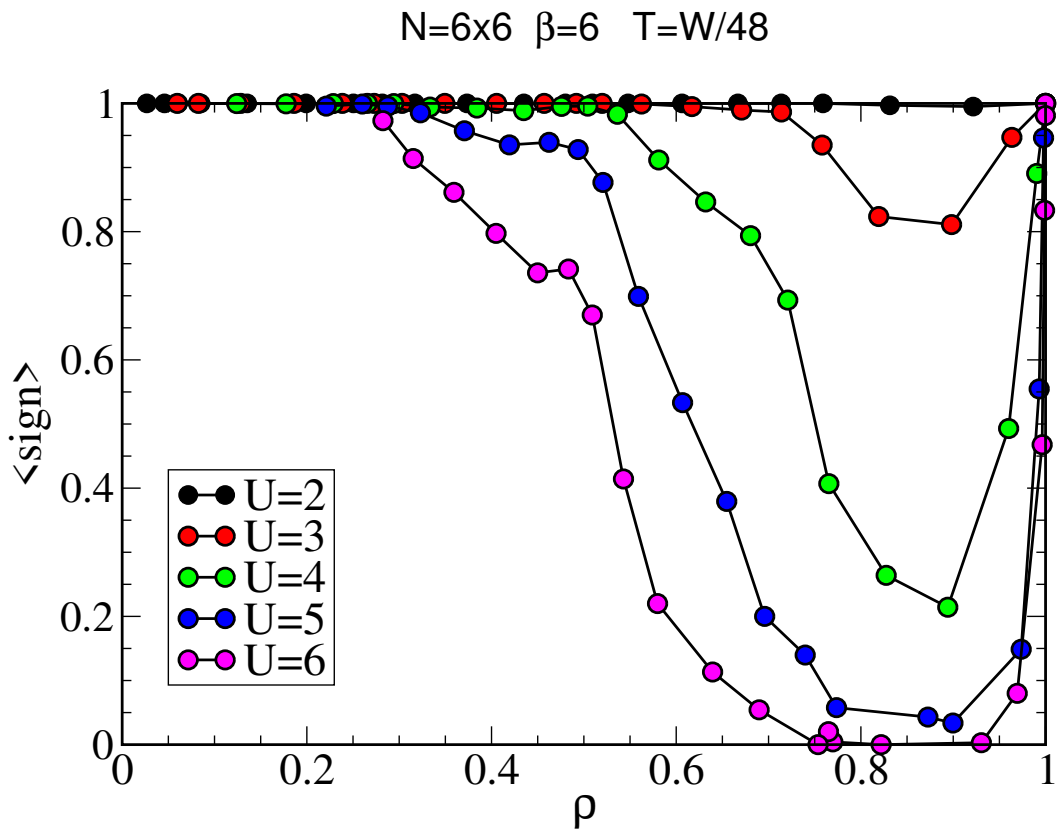

Local measurements converge at relatively high T (before sign problem):

Good quality data for momentum distribution $n(k)$, N=24x24 lattices.

Measurements of long range order generally converge at low T (sign problem present):

d-wave pairing not measurable.

Quantum simulation results for the square lattice Hubbard Hamiltonian at $U = 4t$. $\rho(\mu)$ develops a plateau at half-filling signalling Mott insulator has formed.

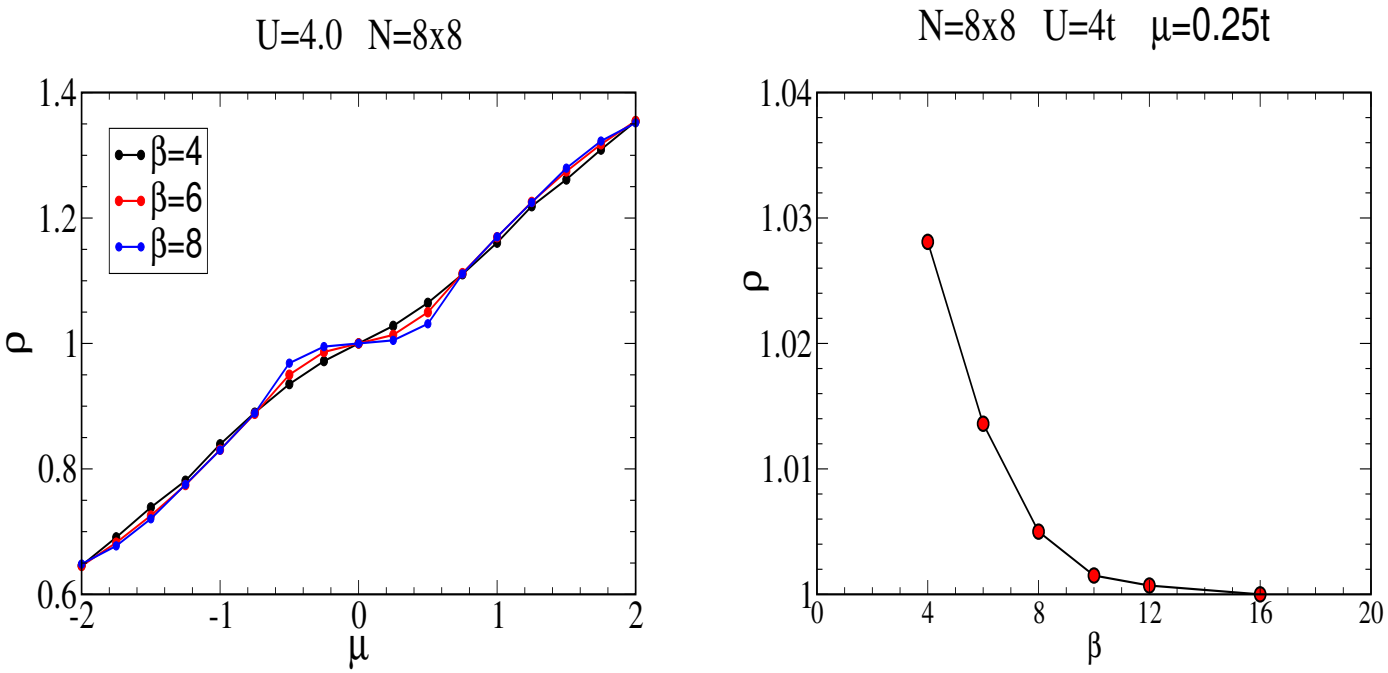

In many situations Slater insulator forming at small U due to the opening of an AF gap, merges smoothly, as U increases, into Mott insulator.

Magnetism at half-filling (no sign problem)

Electron spins on two neighboring sites like to be antiparallel.

Bipartite lattices are a natural for long range antiferromagnetic order

where this up-down pattern extends over entire lattice.

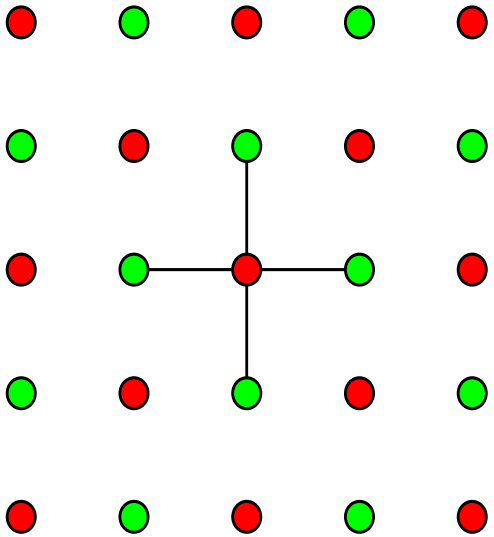

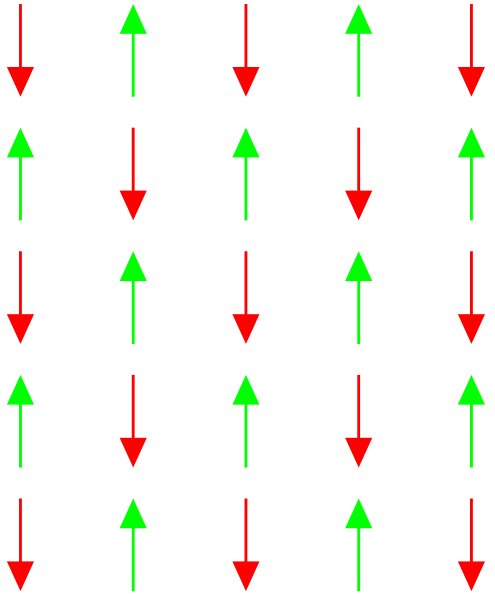

Competing theory:

Anderson: low T phase is resonating valence bond. No LRAFO

DQMC answered this question (in favor of LRAFO).

DQMC Simulation

Antiferromagnetic spin correlations

$$c(l_x, l_y) = \left\langle \left(n_{lx,ly,\uparrow} - n_{lx,ly,\downarrow} \right) \left(n_{0,0,\uparrow} - n_{0,0,\downarrow} \right) \right\rangle$$

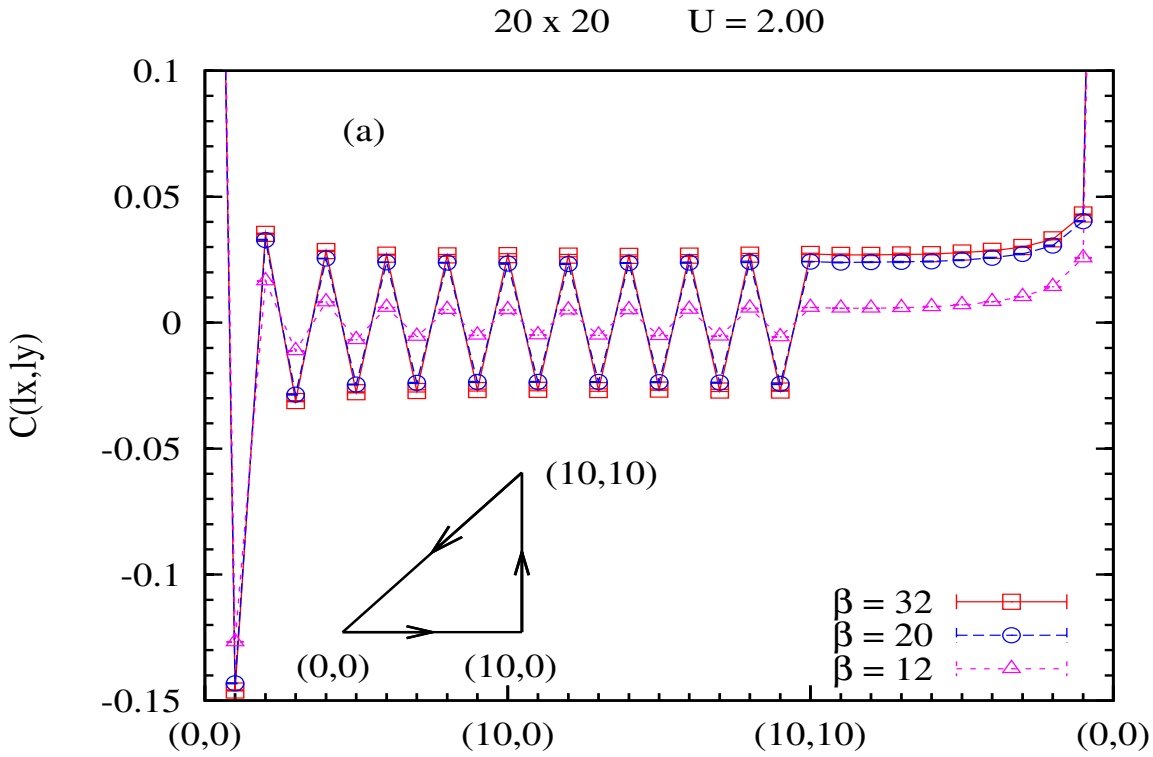

There is long range antiferromagnetic order!

"Quantum Monte Carlo Study of the 2D Fermion Hubbard Model at Half-Filling", C.N. Varney, C.R. Lee, Z.J. Bai, S. Chiesa, M. Jarrell, and RTS, Phys. Rev. B80, 075116 (2009).

DQMC results- Fermi distribution $n(k_x, k_y)$

$U = 2$ Fermi function:

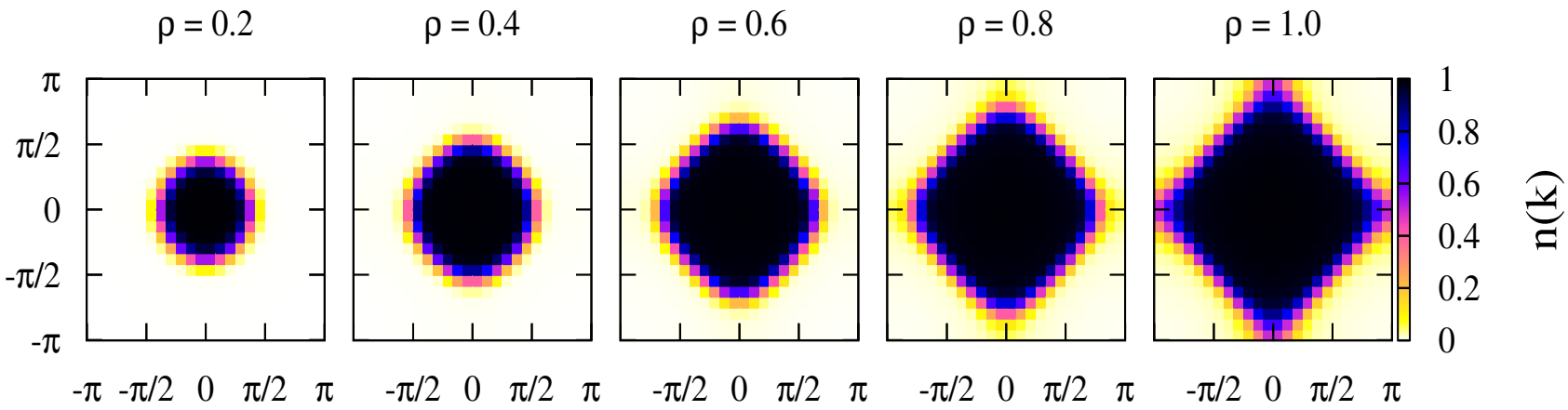

$U = 2$ Gradient of Fermi function:

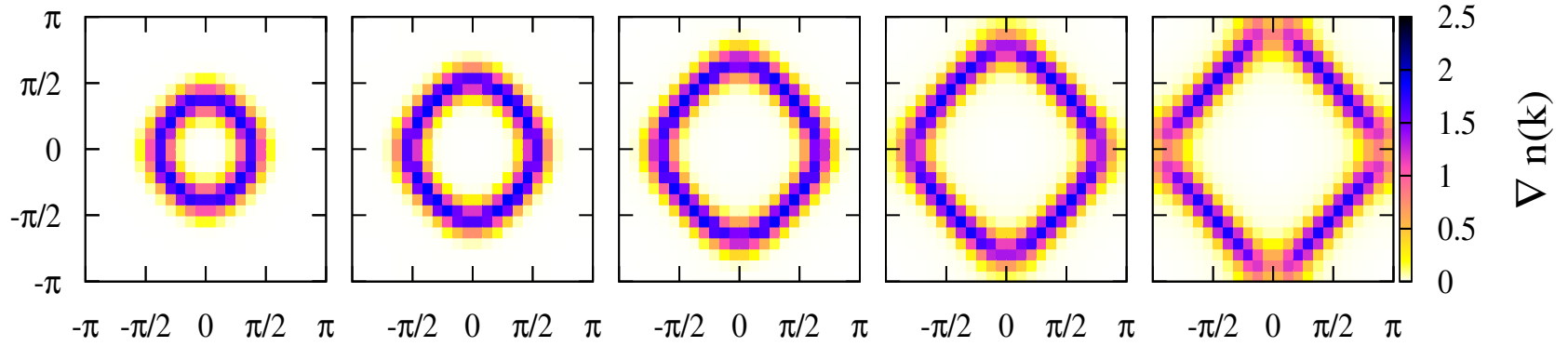

Distinguishing metals and insulators via momentum-resolved spectral function

$$G(\mathbf{q},\tau) = \int_{-\infty}^{+\infty} d\omega \frac{\exp(-\omega\tau)}{1+\exp(-\beta\omega)} A(\mathbf{q},\omega) \qquad N(\omega) = \sum_{\mathbf{q}} A(\mathbf{q},\omega) \ .$$

Square lattice Hubbard Hamiltonian at half-filling:

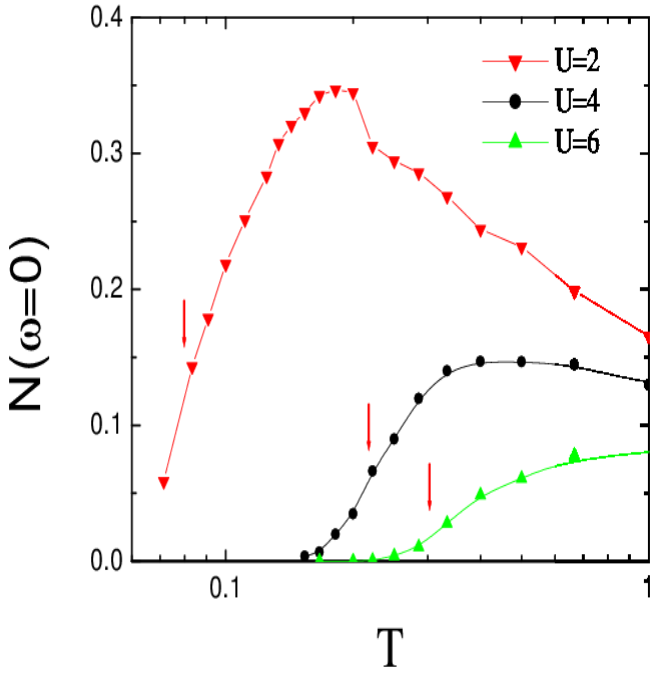

$N(\omega = 0) \to 0$ as $T \to 0$

- Small U: Slater insulator driven by SDW order
- Intermediate U crossover to Mott insulator.

Size of insulating gap $\propto$ temperature range over which $N(\omega = 0) = 0$.

Momentum resolution: Track peak in $A(\mathbf{q},\omega)$ to infer dressed quasiparticle dispersion.

6. Why Ultracold Atoms?

Transition Metal Monoxides - Not really the single band Hubbard model!

Kinetic Energy	$3d$ bandwidth	t_d
Correlation Energy	On-site Coulomb	U_d
Multiple orbitals	Hund's rule (exchange)	J_H
Both Mn and O atoms	Charge transfer energy	$E_{3d} - E_{2p}$
Mn in cubic environment	Crystal field splitting	$E_{e_g} - E_{t_{2g}}$

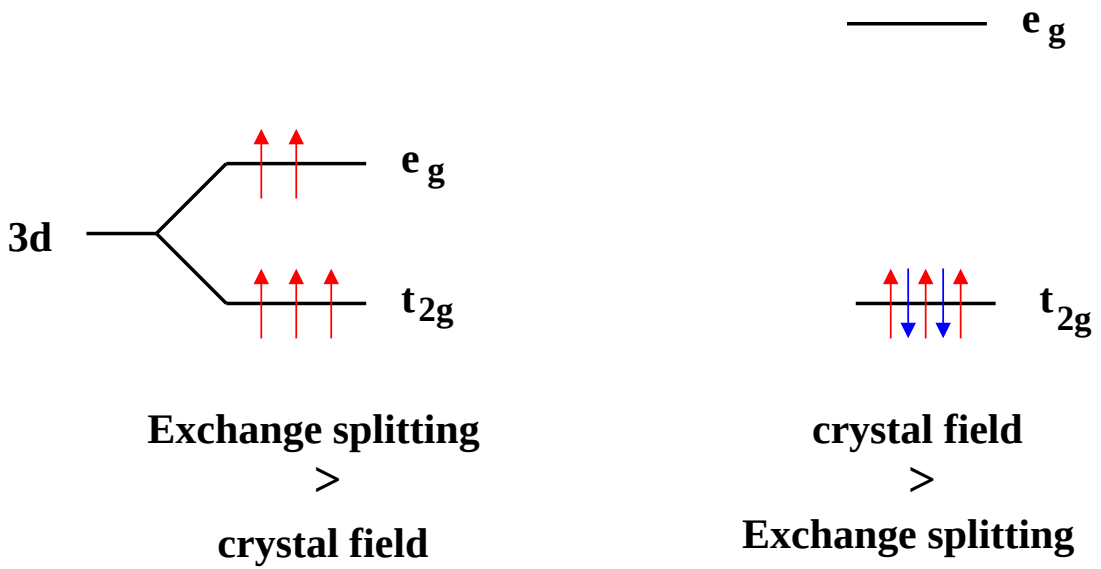

Loss of moment transition actually a "high-spin to low spin transition"?

Crystal field splitting decreases below exchange splitting as pressure applied.

Cuprate Superconductors - Not really the single band Hubbard model!

Again, many 'real life' complications

Like TMOs: Oxygen orbitals. 3-band ('Emery') model.

Charge transfer versus Mott-Hubbard Insulator

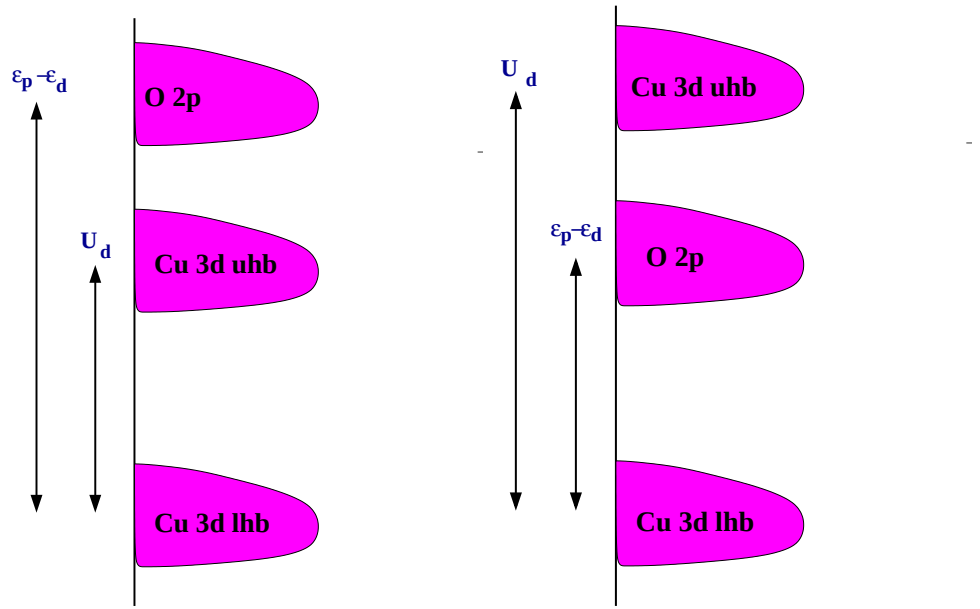

Role of number of layers and interlayer atoms

$La_{1-x}Sr_xCuO_2$: $T_c \approx 35^\circ K$.

$Y_1Ba_2Cu_3O_{7-\delta}$: $T_c \approx 90^\circ K$.

Hubbard Hamiltonian 'particle-hole' symmetry.

Cuprate superconductors: electron doped $\neq$ hole doped.

Role of phonons

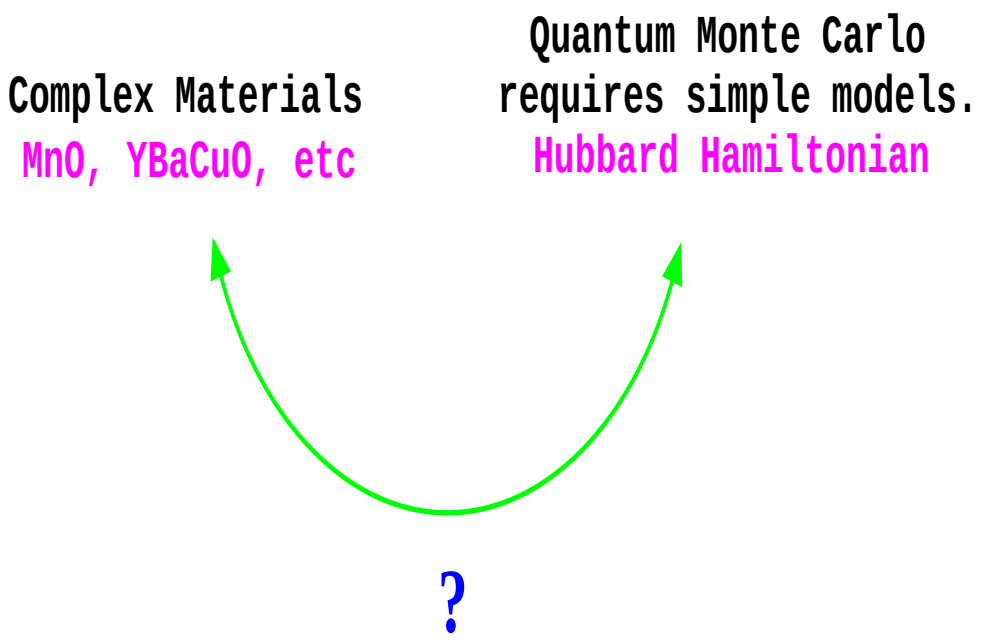

The direct simulation of quantum systems on classical computers is very difficult because of the huge amount of memory required to store the explicit state of the quantum system. This is due to the fact that quantum states are described by a number of parameters that grows exponentially with the system size.

Iulia Buluta and Franco Nori, Quantum Simulators Science 326 pp.108-111, (2009). DOI: 10.1126/science.1177838

If no sign problem, DQMC is power law $o(N^3)$.

But, most interesting models have a bad sign problem!

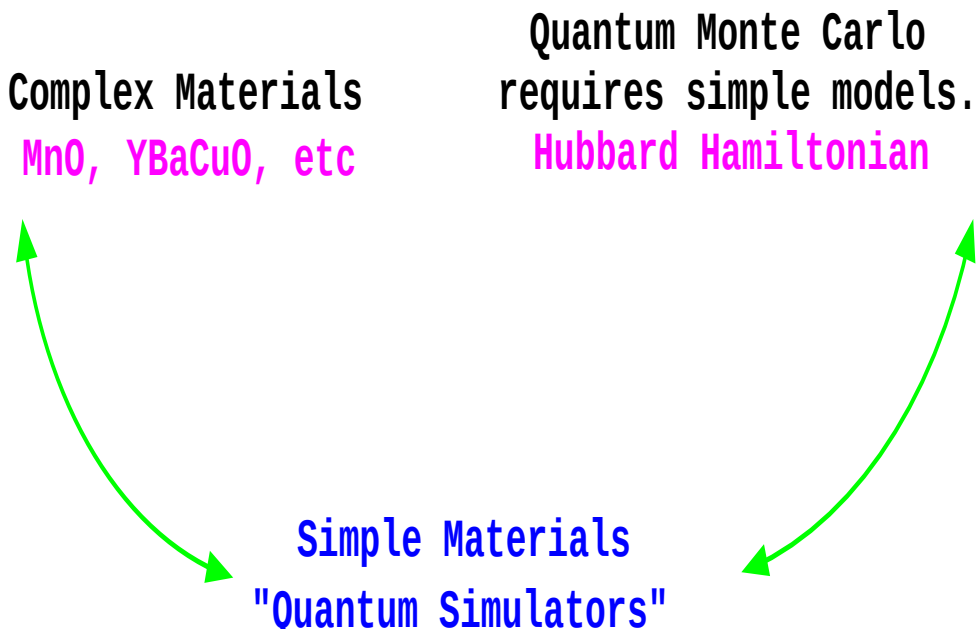

Quantum simulators are controllable quantum systems that can be used to simulate other quantum systems.

Iulia Buluta and Franco Nori, Quantum Simulators Science 326 pp.108-111, (2009). DOI: 10.1126/science.1177838

Ultra-cold atoms!

Optical Lattices

Lattice formed by interference of counterpropagating laser beams.
Atoms $\left(o(10^5)\right)$ trapped by Stark shift. Cool evaporatively $\cdots$.
Different geometries accessable (e.g. cubic, honeycomb, $\cdots$)

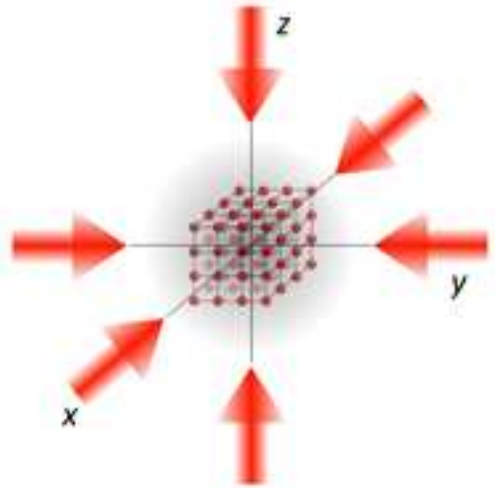

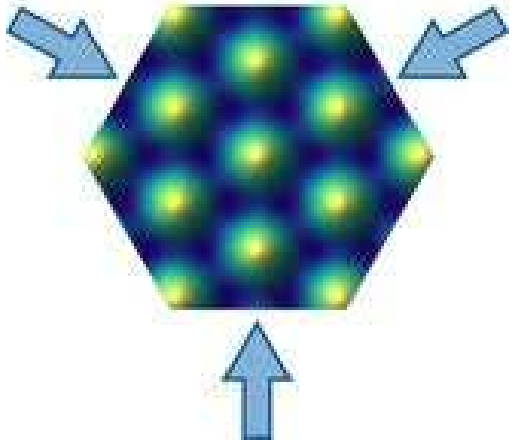

Control hopping t, interactions U
much more easily than solids.
Use, e.g. to drive Mott insulator.

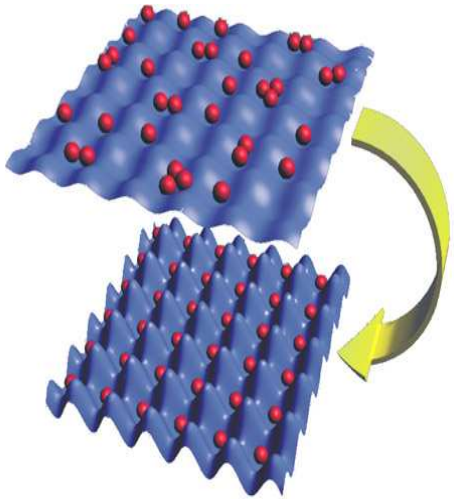

Tune laser wavelength
or Feshbach resonance.

Quantum Monte Carlo Simulations of Hubbard Model with Confining potential.

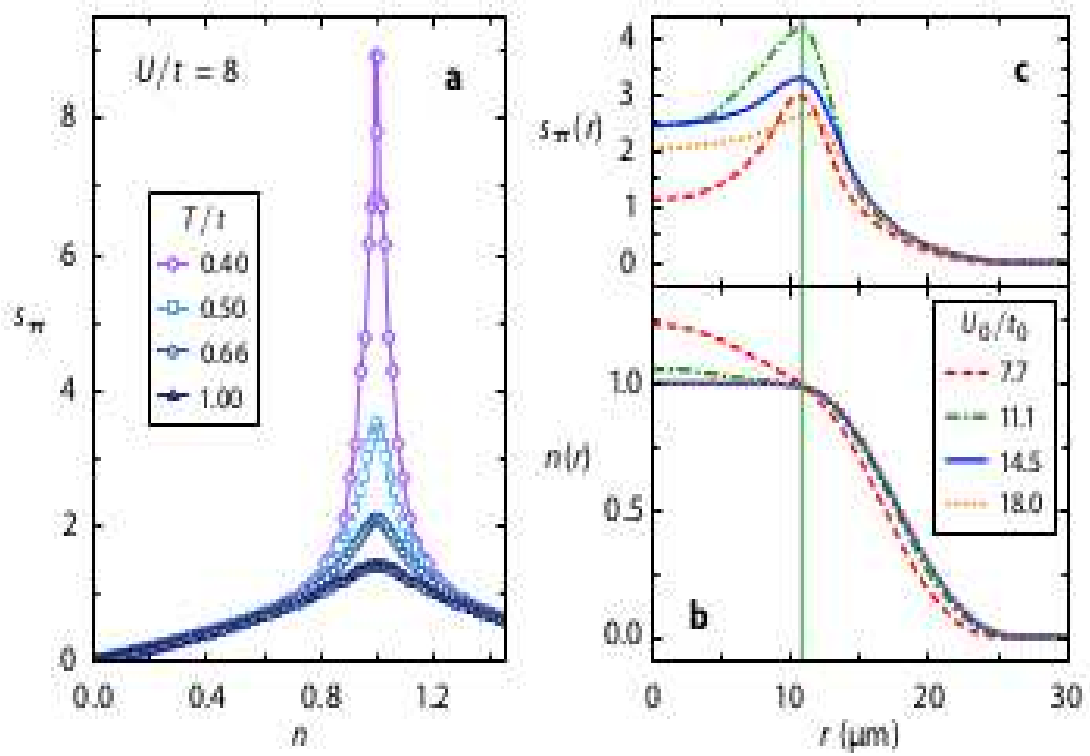

Illustrates first challenge: Confining potential leads to inhomogeneous density.

Local Mott/AF regions coexist with paramagnetic metal.

How to disentangle?

"Observation of antiferromagnetic correlations in the Hubbard model with ultracold atoms", R.A. Hart, P.M. Duarte, T. Yang, X. Liu, T. Paiva, E. Khatami, RTS, N. Trivedi, D.A. Huse and R.G. Hulet, Nature 519, 211 (2015).

"Compressibility of a fermionic Mott insulator of ultracold atoms," P.M. Duarte, R.A. Hart, T-L. Yang, X. Liu, T. Paiva, E. Khatami, RTS, N. Trivedi, and R.G. Hulet, Phys. Rev. Lett. 114, 070403 (2015).

Comparison of experiment and Quantum Monte Carlo

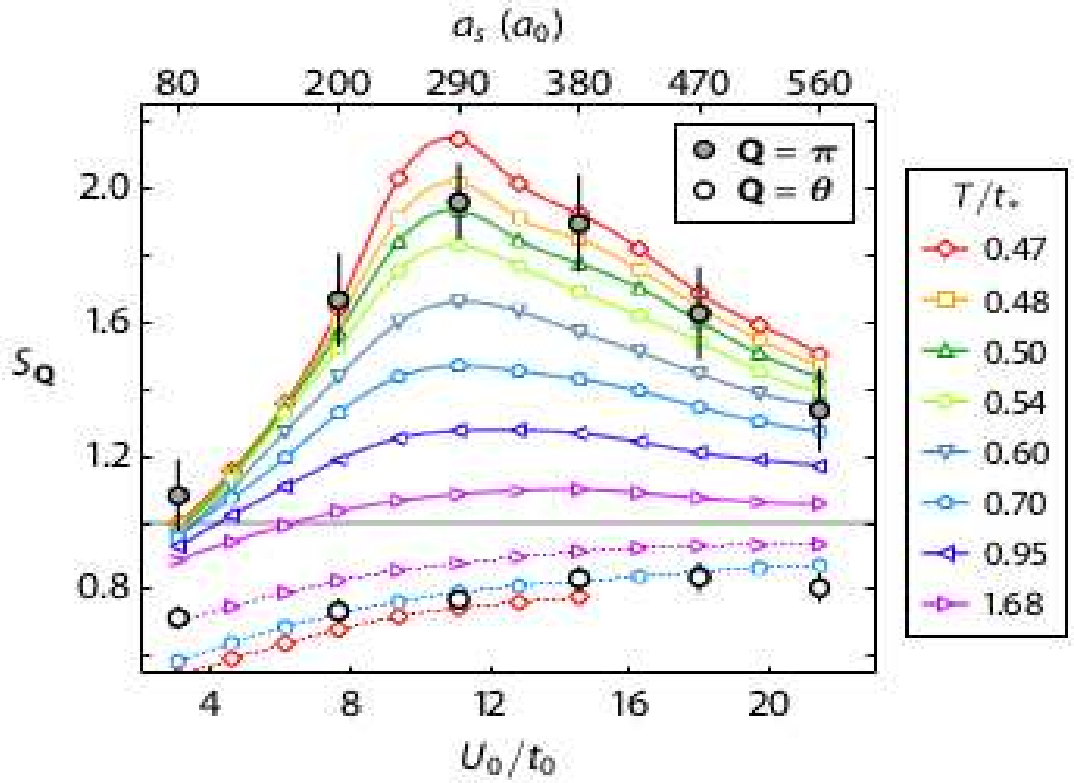

Illustrates second challenge:

Limitations on ability to cool.

Temperatures: nanoKelvins, but so are hopping t and interaction U:

Comparison with QMC provides thermometer.

$\Rightarrow$ T/t is not small!

7. Outlook

(My particular interests $\cdots$)

- Cold atom experimentalists have some work to do: Lower T
- SU(N) Hubbard models

Hazzard, Padilla, Takahashi, Taie, Nishizawa, Takusa, Kuno, Wei

- Electron-Phonon Models

Yuxi Zhang, Cohen-Stead, Mondaini, Barros, Batrouni, Bradley, Feng

- Langevin Methods

Cohen-Stead, Barros, Batrouni